

Supersymmetry and FCNC Effects

Mikołaj Misiak, Stefan Pokorski and Janusz Rosiek

*Institute of Theoretical Physics, Warsaw University,
Hoża 69, 00-681 Warsaw, Poland*

Abstract

We consider Flavour Changing Neutral Current processes in the framework of the supersymmetric extension of the Standard Model. FCNC constraints on the structure of sfermion mass matrices are reviewed. Furthermore, we analyze supersymmetric contributions to FCNC transitions which remain in the limit of flavour-conserving sfermion mass matrices. Implications of the FCNC constraints on the structure of sfermion mass matrices for SUSY breaking and sfermion mass generation are discussed. We conclude that the supersymmetric flavour problem is intriguing but perhaps not as severe as it is commonly believed.

To appear in the Review Volume “Heavy Flavours II”, eds. A.J. Buras and M. Lindner, Advanced Series on Directions in High Energy Physics, World Scientific Publishing Co., Singapore.

1 Introduction.

Gauge invariance, renormalizability and particle content of the Standard Model imply the absence (in the lepton sector) or strong suppression (in the quark sector) of the Flavour Changing Neutral Current (FCNC) transitions. Such transitions in the quark sector are absent at the tree level. At one-loop, they are suppressed by light quark masses (when compared to M_W) and by small mixing between the third and the first two generations. The predicted suppression of the FCNC processes is in beautiful agreement with the presently available experimental data. However, the Standard Model is very likely to be only an effective “low energy” theory which, up to some scale Λ , is a good approximation to the deeper (and yet unknown) theory of fundamental interactions. In such a case, renormalizable interactions of the Standard Model are in general supplemented by higher dimensional interaction terms suppressed by some powers of the scale Λ . These new interactions depend on the structure of the more fundamental theory. Their $SU(3) \times SU(2) \times U(1)$ invariance is not sufficient any more to protect the observed strong suppression of the FCNC processes. Consistency with the data then require that either the scale Λ is huge or dangerous new interactions are absent because of symmetries of the deeper theory.

The Minimal Supersymmetric Standard Model (MSSM) contains the new scale Λ which is the scale of soft supersymmetry breaking. It is expected to be of the order of 1 TeV, so long as supersymmetry is the solution to the so-called hierarchy problem. That low scale of new physics together with a fully unconstrained renormalizable minimal² supersymmetric extension of the SM would be disastrous for the FCNC transitions.

As we shall see in the next section, in the MSSM there are, broadly speaking, two kinds of new contributions to the FCNC transitions. First of all, they may originate

² By minimal extension we mean the following three assumptions:
(i) minimal particle content consistent with observed SM particles and SUSY,
(ii) $SU(3) \times SU(2) \times U(1)$ gauge invariance,
(iii) most general soft ($\dim < 4$) SUSY breaking terms consistent with $SU(3) \times SU(2) \times U(1)$ invariance.

from flavour mixing in the sfermion mass matrices [1]. However, even in the absence of such genuinely new effects, i.e. assuming that the Kobayashi-Maskawa matrix is solely responsible for flavour mixing, new contributions arise from charged Higgs boson and chargino exchanges.

Given the strong suppression of the FCNC transitions observed in Nature, it is very interesting to study the resulting upper bounds on flavour changing elements in the sfermion mass matrices and on the splitting among their diagonal elements. Although these are free parameters of the MSSM, ultimately their values have to be obtained from a theory of soft supersymmetry breaking and/or fermion mass generation. Therefore, such bounds may provide important hints towards such a theory. As we shall see, indeed, the sfermion mass matrices are strongly constrained both in their flavour diagonal and off-diagonal elements. The weakest are the constraints on the third generation sfermion masses.

Since, at the same time, the third generation sfermions and chargino are expected to be among the lightest superpartners, also the following question is of obvious interest: Suppose that flavour mixing in the sfermion mass matrices is small and can be neglected. The potential impact of supersymmetry on the FCNC transitions appears then solely through the KM angles present in flavour changing vertices, i.e. it is due to the charged Higgs and chargino-squark contributions. Deviations from the SM would be then most probably first observed in $\bar{K}^0 K^0$ (ϵ_K parameter), $\bar{B}^0 B^0$ and $\bar{D}^0 D^0$ mixing, as well as the $b \rightarrow s\gamma$ transition. Furthermore, it is reasonable to assume that the first two generations of sfermions are heavy and degenerate in mass, and to study the effects which can be generated by light chargino, charged Higgs boson and the third generation of sfermions. As we shall see, such a study has also interesting model independent aspects.

We find it useful to organize this text according to the two questions asked above. In section 2, we briefly introduce the necessary part of the MSSM notation. In section 3, limits on flavour violation in the sfermion mass matrices are discussed. In section 4, we consider supersymmetric contributions to the FCNC effects from the chargino–stop (charged Higgs boson – top) loops, assuming no new sources of

flavour mixing in the sfermion mass matrices. Finally, in section 5, we present a brief discussion of the implications of FCNC on problems like the pattern of soft supersymmetry breaking or sfermion mass generation.

2 Formalism and notation.

We start with a brief description of the MSSM and with establishing our notation conventions which are similar to the ones used in ref. [2]. The MSSM matter fields are in the following representations of the $SU(3) \times SU(2) \times U(1)$ gauge group:³

$$\begin{array}{ccccccc}
(1, 2, -\frac{3}{10}) & (1, 1, \frac{3}{5}) & (3, 2, \frac{1}{10}) & (\bar{3}, 1, \frac{1}{5}) & (\bar{3}, 1, -\frac{2}{5}) & (1, 2, -\frac{3}{10}) & (1, 2, \frac{3}{10}) \\
L^I & E^I & Q^I & D^I & U^I & H^1 & H^2 \\
\Psi_L^I & \Psi_E^I & \Psi_Q^I & \Psi_D^I & \Psi_U^I & \Psi_H^1 & \Psi_H^2
\end{array}$$

Capital letters in the second row denote complex scalar fields. The fields in the third row are left-handed fermions. The upper index $I = 1, 2, 3$ labels the generations. Lower indices (when present) will label components of $SU(2)$ -doublets. Two $SU(2)$ -doublets can be contracted into an $SU(2)$ -singlet, e.g. $H^1 H^2 = -H_1^1 H_2^2 + H_2^1 H_1^2$.

The supersymmetric part of the MSSM Lagrangian schematically appears as

$$\begin{aligned}
\mathcal{L}_{SUSY} = & -\frac{1}{4} F_G^{a\mu\nu} F_G^a_{\mu\nu} + i\bar{\lambda}_G^a \not{D}_{ab} \lambda_G^b + (D^\mu \phi)^\dagger (D_\mu \phi) + i\bar{\psi} \not{D} \psi \\
& - \left(\frac{\partial \tilde{W}}{\partial \phi_i} \right)^* \left(\frac{\partial \tilde{W}}{\partial \phi_i} \right) - \frac{1}{2} \left(\frac{\partial^2 \tilde{W}}{\partial \phi_i \partial \phi_j} \psi_i^T C \psi_j + \text{h.c.} \right) \\
& - \sqrt{2} g_G \left(\phi^\dagger T_G^a \lambda_G^a C \psi + \text{h.c.} \right) - \frac{1}{2} g_G^2 (\phi^\dagger T_G^a \phi) (\phi^\dagger T_G^a \phi). \quad (1)
\end{aligned}$$

where

$$\tilde{W} = \mu H^1 H^2 + Y_l^{IJ} H^1 L^I E^J + Y_d^{IJ} H^1 Q^I D^J + Y_u^{IJ} H^2 Q^I U^J \quad (2)$$

In eq. (1), the index G labels the color, weak isospin and hypercharge factors in the Standard Model gauge group, and indices a and b range over adjoint representations of the nonabelian subgroups. All MSSM scalars are assembled into ϕ , while matter fermions and gauginos are respectively contained within the four-component left handed ψ and λ fields. The charge conjugation matrix is denoted by C .

³ The $U(1)$ charges are given in the $SU(5)$ normalization.

Apart from the three gauge coupling constants, the supersymmetric part of the MSSM Lagrangian depends on the Yukawa coupling matrices $Y_{l,d,u}$ and on the parameter μ which multiplies the first term in eq. (2).

The remaining part of the MSSM Lagrangian consists of the soft supersymmetry breaking terms: gaugino masses, scalar masses and trilinear scalar interactions

$$\begin{aligned} \mathcal{L}_{soft} = & -\frac{1}{2} \left(M_3 \tilde{g}^{aT} C \tilde{g}^a + M_2 \tilde{W}^{iT} C \tilde{W}^i + M_1 \tilde{B}^T C \tilde{B} + \text{h.c.} \right) \\ & - M_{H^1}^2 H^{1\dagger} H^1 - M_{H^2}^2 H^{2\dagger} H^2 - L^{I\dagger} (M_L^2)^{IJ} L^J - E^{I\dagger} (M_E^2)^{IJ} E^J \\ & - Q^{I\dagger} (M_Q^2)^{IJ} Q^J - D^{I\dagger} (M_D^2)^{IJ} D^J - U^{I\dagger} (M_U^2)^{IJ} U^J \\ & + \left(A_E^{IJ} H^1 L^J E^I + A_D^{IJ} H^1 Q^J D^I + A_U^{IJ} H^2 Q^J U^I + B \mu H^1 H^2 + \text{h.c.} \right). \end{aligned} \quad (3)$$

Assuming the above form of the soft supersymmetry breaking terms, we depart from full generality. In principle, \mathcal{L}_{soft} could be supplemented by all the bilinear and trilinear scalar interaction terms present in eq. (1), but with coupling constants unrelated to those in eq. (2). Here, we follow the standard approach and assume absence of such terms. Such an assumption is consistent with renormalization: So long as these terms are absent at the tree level, they are not generated via loops to all orders in perturbation theory.

In the physically acceptable regions of the parameter space, vacuum expectation values are developed only by the Higgs scalars

$$\langle H^1 \rangle = \begin{pmatrix} \frac{v_1}{\sqrt{2}} \\ 0 \end{pmatrix} \equiv \begin{pmatrix} \frac{v \cos \beta}{\sqrt{2}} \\ 0 \end{pmatrix}, \quad \langle H^2 \rangle = \begin{pmatrix} 0 \\ \frac{v_2}{\sqrt{2}} \end{pmatrix} \equiv \begin{pmatrix} 0 \\ \frac{v \sin \beta}{\sqrt{2}} \end{pmatrix}. \quad (4)$$

The value of $v \simeq 246$ GeV is determined from the W -boson mass in the same way as in the Standard Model.

Lepton and quark mass eigenstates are obtained from the original left-handed fermion fields with help of 3×3 unitary matrices $V_{L,R}^{E,U,D}$ as follows:

$$\begin{aligned} \nu &= V_L^E \Psi_{L1}, & u &= V_L^U \Psi_{Q1} + V_R^U C \bar{\Psi}_U^T, \\ e &= V_L^E \Psi_{L2} + V_R^E C \bar{\Psi}_E^T, & d &= V_L^D \Psi_{Q2} + V_R^D C \bar{\Psi}_D^T. \end{aligned} \quad (5)$$

Their diagonal 3×3 mass matrices read

$$m_e = -\frac{v \cos \beta}{\sqrt{2}} V_R^E Y_e^T V_L^{E\dagger}, \quad m_u = \frac{v \sin \beta}{\sqrt{2}} V_R^U Y_u^T V_L^{U\dagger}, \quad m_d = -\frac{v \cos \beta}{\sqrt{2}} V_R^D Y_d^T V_L^{D\dagger},$$

As in the Standard Model, the Kobayashi-Maskawa matrix is $K = V_L^U V_L^D{}^\dagger$.

Diagonalization of the scalar mass matrices usually proceeds in two steps. First, the squarks and sleptons are rotated ‘‘parallel’’ to their fermionic superpartners

$$\tilde{N}^0 = V_L^E L_1, \quad \tilde{L}^0 = \begin{pmatrix} V_L^E L_2 \\ V_R^E E^\star \end{pmatrix}, \quad \tilde{U}^0 = \begin{pmatrix} V_L^U Q_1 \\ V_R^U U^\star \end{pmatrix}, \quad \tilde{D}^0 = \begin{pmatrix} V_L^D Q_2 \\ V_R^D D^\star \end{pmatrix}. \quad (6)$$

The fields in the l.h.s of the above equations form the so-called ‘‘super-KM’’ basis in the space of MSSM scalars. These fields may be often more convenient to work with, even though they are not mass eigenstates. Their mass matrices have the following form:

$$\begin{aligned} \mathcal{M}_{\tilde{U}}^2 &= \begin{pmatrix} (M_{\tilde{U}}^2)_{LL} + m_u^2 - \frac{\cos 2\beta}{6}(M_Z^2 - 4M_W^2)\hat{1} & (M_{\tilde{U}}^2)_{LR} - \cot \beta \mu m_u \\ (M_{\tilde{U}}^2)_{LR}^\dagger - \cot \beta \mu^\star m_u & (M_{\tilde{U}}^2)_{RR} + m_u^2 + \frac{2\cos 2\beta}{3}M_Z^2 \sin^2 \theta_W \hat{1} \end{pmatrix}, \\ \mathcal{M}_{\tilde{D}}^2 &= \begin{pmatrix} (M_{\tilde{D}}^2)_{LL} + m_d^2 - \frac{\cos 2\beta}{6}(M_Z^2 + 2M_W^2)\hat{1} & (M_{\tilde{D}}^2)_{LR} - \tan \beta \mu m_d \\ (M_{\tilde{D}}^2)_{LR}^\dagger - \tan \beta \mu^\star m_d & (M_{\tilde{D}}^2)_{RR} + m_d^2 - \frac{\cos 2\beta}{3}M_Z^2 \sin^2 \theta_W \hat{1} \end{pmatrix}, \\ \mathcal{M}_{\tilde{L}}^2 &= \begin{pmatrix} (M_{\tilde{L}}^2)_{LL} + m_l^2 + \frac{\cos 2\beta}{2}(M_Z^2 - 2M_W^2)\hat{1} & (M_{\tilde{L}}^2)_{LR} - \tan \beta \mu m_l \\ (M_{\tilde{L}}^2)_{LR}^\dagger - \tan \beta \mu^\star m_l & (M_{\tilde{L}}^2)_{RR} + m_l^2 - \cos 2\beta M_Z^2 \sin^2 \theta_W \hat{1} \end{pmatrix}, \\ \mathcal{M}_{\tilde{N}}^2 &= V_L^E M_E^2 V_L^{E\dagger} + \frac{\cos 2\beta}{2} M_Z^2 \hat{1}, \end{aligned} \quad (7)$$

where θ_W is the Weinberg angle, $\hat{1}$ stands for the 3×3 unit matrix, and the flavour-changing entries are contained in

$$\begin{aligned} (M_{\tilde{U}}^2)_{LL} &= V_L^U M_Q^2 V_L^{U\dagger} & (M_{\tilde{U}}^2)_{RR} &= V_R^U M_U^{2T} V_R^{U\dagger} & (M_{\tilde{U}}^2)_{LR} &= -\frac{v \sin \beta}{\sqrt{2}} V_L^U A_U^\star V_R^{U\dagger} \\ (M_{\tilde{D}}^2)_{LL} &= V_L^D M_Q^2 V_L^{D\dagger} & (M_{\tilde{D}}^2)_{RR} &= V_R^D M_D^{2T} V_R^{D\dagger} & (M_{\tilde{D}}^2)_{LR} &= \frac{v \cos \beta}{\sqrt{2}} V_L^D A_D^\star V_R^{D\dagger} \\ (M_{\tilde{L}}^2)_{LL} &= V_L^E M_L^2 V_L^{E\dagger} & (M_{\tilde{L}}^2)_{RR} &= V_R^E M_E^{2T} V_R^{E\dagger} & (M_{\tilde{L}}^2)_{LR} &= \frac{v \cos \beta}{\sqrt{2}} V_L^E A_E^\star V_R^{E\dagger}. \end{aligned} \quad (8)$$

It often happens that certain FCNC processes are sensitive to particular entries in the above nine matrices. For $(M_{\tilde{U}}^2)_{LL}$, we will denote these entries as follows:

$$(M_{\tilde{U}}^2)_{LL} = \begin{pmatrix} (m_{U1}^2)_{LL} & (\Delta_U^{12})_{LL} & (\Delta_U^{13})_{LL} \\ (\Delta_U^{21})_{LL} & (m_{U2}^2)_{LL} & (\Delta_U^{23})_{LL} \\ (\Delta_U^{31})_{LL} & (\Delta_U^{32})_{LL} & (m_{U3}^2)_{LL} \end{pmatrix}, \quad (9)$$

and analogously for all the other matrices. (Of course $\Delta_{LL}^{IJ} = \Delta_{LL}^{JI^*}$ and $\Delta_{RR}^{IJ} = \Delta_{RR}^{JI^*}$, but no such relation holds for Δ_{LR} .) Experimental constraints will be given on the flavour-changing mass insertions normalized to a geometric average of the diagonal entries, e.g.

$$(\delta_U^{IJ})_{LR} = \frac{(\Delta_U^{IJ})_{LR}}{(m_{UI})_{LL} (m_{UJ})_{RR}}. \quad (10)$$

Two remarks are in order here. First, let us suppose that we have a theory of fermion and sfermion masses which are fixed in some electroweak basis. We see then, that all four rotations V_L^U, V_L^D, V_R^U and V_R^D (not just K) become partly “observables” through the sfermion mass matrices⁴.

Secondly, one should remember that the matrix M_Q^2 is common to the up and down sectors, because of the $SU(2)$ gauge invariance. Therefore

$$(M_U^2)_{LL} = K(M_D^2)_{LL}K^\dagger \quad (11)$$

This means that it is impossible to set all the $(\delta^{IJ})_{LL}$ to zero simultaneously, unless $M_Q^2 \sim \hat{1}$, which implies $(M_U^2)_{LL} = (M_D^2)_{LL} \sim \hat{1}$.

Matrices \mathcal{M}_U^2 and \mathcal{M}_D^2 can be diagonalized by two additional 6×6 unitary matrices Z_U and Z_D , respectively

$$(\mathcal{M}_U^2)^{diag} = Z_U^\dagger \mathcal{M}_U^2 Z_U \quad (12)$$

$$(\mathcal{M}_D^2)^{diag} = Z_D^T \mathcal{M}_D^2 Z_D^* \quad (13)$$

Of course, if all δ^{IJ} were zero (i.e. if there was no flavour mixing in the “super-KM” basis), then the matrices Z_U and Z_D would preserve flavour. Possible off-diagonal entries in these matrices would then correspond to left-right mixing, i.e. mixing between superpartners of left- and right-handed quarks having the same flavour.

Flavour changing interactions of physical sfermions (mass eigenstates) depend on the rotations Z ’s as well as on the mixing between gauginos and higgsinos. The physical Dirac chargino and Majorana neutralino eigenstates are linear combinations

⁴ except for “singular” cases when the sfermion mass matrices are diagonal and degenerate or completely aligned with squared Yukawa coupling matrices in the weak eigenstate basis.

of left-handed Winos, Binos and Higgsinos

$$\chi^- = (Z^-)^\dagger \begin{pmatrix} \tilde{W}^- \\ (\Psi_H^1)_2 \end{pmatrix} + (Z^+)^T \begin{pmatrix} C\overline{\tilde{W}^+}^T \\ C(\overline{\Psi_H^2})_1^T \end{pmatrix} \quad (14)$$

$$\chi^0 = Z_N^\dagger \begin{pmatrix} \tilde{B} \\ \tilde{W}_3 \\ (\Psi_H^1)_1 \\ (\Psi_H^2)_2 \end{pmatrix} + Z_N^T \begin{pmatrix} C\overline{\tilde{B}}^T \\ C\overline{\tilde{W}_3}^T \\ C(\overline{\Psi_H^1})_1^T \\ C(\overline{\Psi_H^2})_2^T \end{pmatrix}. \quad (15)$$

The unitary transformations Z^+ , Z^- and Z_N diagonalize mass matrices of these fields

$$\mathcal{M}_{\chi^\pm} = (Z^-)^T \begin{pmatrix} M_2 & \sqrt{2}M_W \sin \beta \\ \sqrt{2}M_W \cos \beta & \mu \end{pmatrix} Z^+ \quad (16)$$

and

$$\mathcal{M}_{\chi^0} = Z_N^T \begin{pmatrix} M_1 & 0 & -M_Z \sin \theta_W \cos \beta & M_Z \sin \theta_W \sin \beta \\ 0 & M_2 & M_Z \cos \theta_W \cos \beta & -M_Z \cos \theta_W \sin \beta \\ -M_Z \sin \theta_W \cos \beta & M_Z \cos \theta_W \cos \beta & 0 & -\mu \\ M_Z \sin \theta_W \sin \beta & -M_Z \cos \theta_W \sin \beta & -\mu & 0 \end{pmatrix} Z_N. \quad (17)$$

The most relevant flavour changing vertices for our further discussion are the ones in which both quarks and squarks are present. There are three types of such vertices: $f\tilde{f}\chi^-$, $f\tilde{f}\chi^0$ and $f\tilde{f}\tilde{g}$. They are presented in Figs. 1-3.

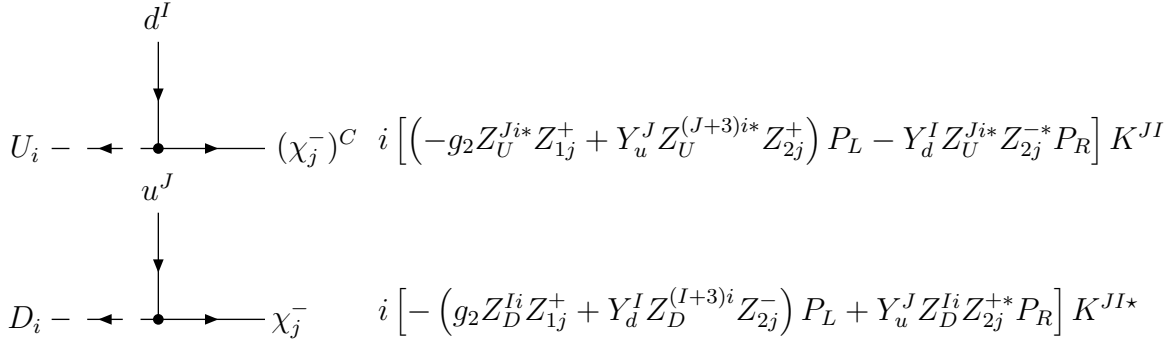


Figure 1: Chargino-quark-squark vertices.

As an example of how these vertices enter FCNC amplitudes, let us list supersymmetric contributions to the $\bar{K}^0 K^0$ mixing. All the MSSM diagrams are shown in Fig. 4. In addition to the Standard Model ($W - q$) box diagrams, we have the charged Higgs, chargino, neutralino and gluino exchanges. In these diagrams, all

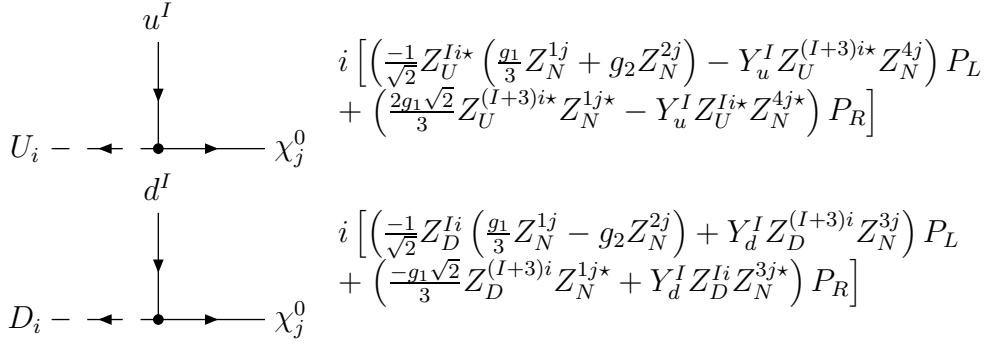


Figure 2: Neutralino-quark-squark vertices.

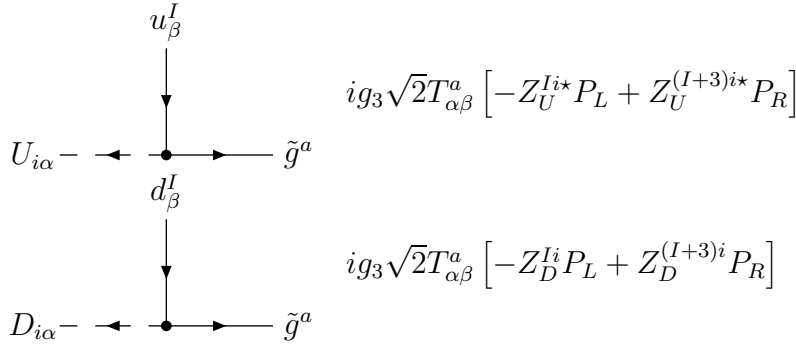
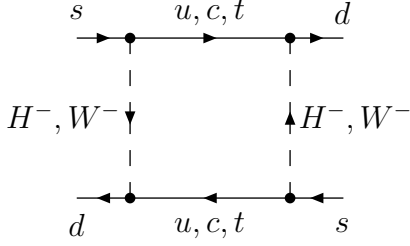


Figure 3: Gluino-quark-squark vertices.

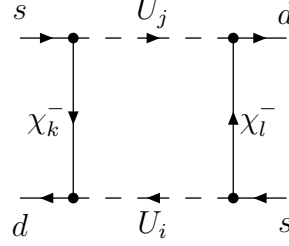
the particles are mass eigenstates, and the vertices depend on the rotations Z_U and Z_D .

It is often convenient to work in the super-KM basis, provided an approximation to the first nonvanishing order in Δ^{IJ} is sufficient. In such a basis, for instance, the diagram (B) in Fig. 4 is replaced by its expansion shown in Fig. 5. In Fig. 5, the fields $\tilde{U}^0 = (\tilde{U}_L^0, \tilde{U}_R^0)$ and $\tilde{C}^0 = (\tilde{C}_L^0, \tilde{C}_R^0)$ are up-squark fields in the super-KM basis, and the vertices are given by the formulae in Figs. 1-2, with flavour-preserving Z_U and Z_D . Similarly, in the super-KM basis, the diagram (C) in Fig. 4 is replaced by its expansion plotted in Fig. 6.

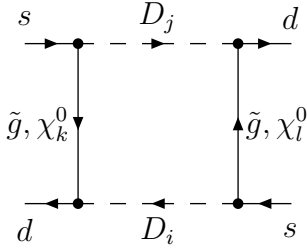
Two important remarks at this point are the following: As we have already said in the introduction, supersymmetric contributions to the FCNC transitions arise even when fermion and sfermion mass matrices are simultaneously flavour-conserving ($\Delta^{IJ} = 0$). These contributions originate from the charged Higgs and chargino exchange diagrams in Fig. 4, with the KM angles in the vertices. Similar diagrams contribute to the $\bar{B}^0 B^0$ and $\bar{D}^0 D^0$ mixing.



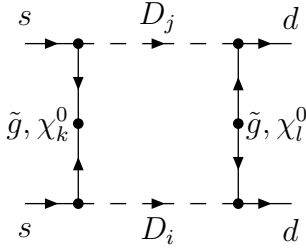
(A): W and charged Higgs exchanges



(B): chargino exchange



(C): neutralino and gluino exchanges



(D): neutralino and gluino exchanges

Figure 4: MSSM diagrams contributing to $\bar{K}^0 K^0$ mixing (crossed diagrams not plotted).

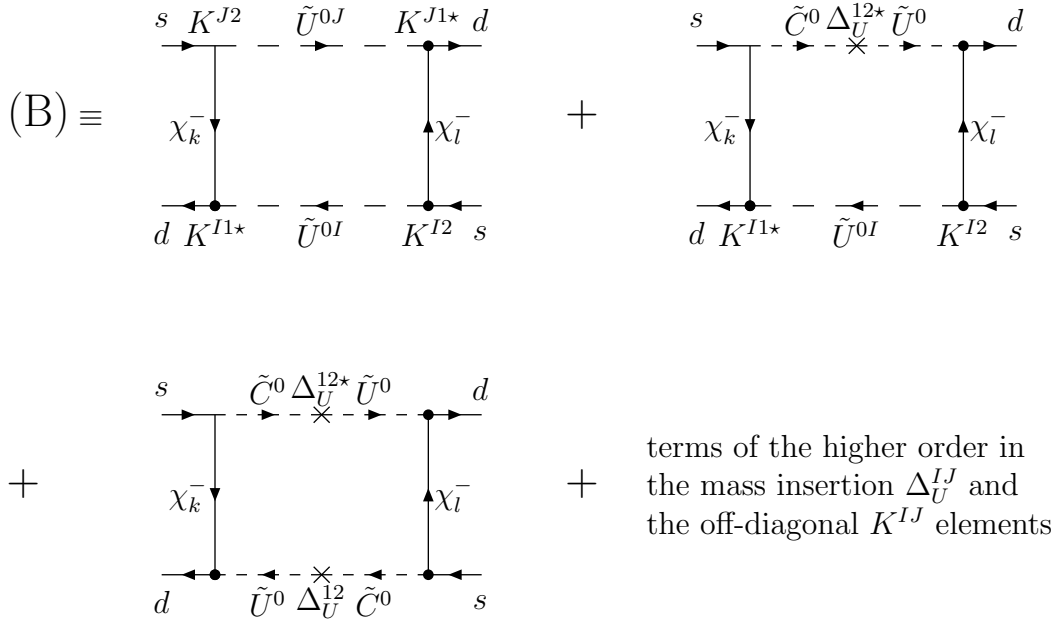


Figure 5: Chargino contribution to $\bar{K}^0 K^0$ in mass insertion expansion.

$$\begin{array}{c}
\begin{array}{c}
s \xrightarrow{\quad} \text{---} \xrightarrow{\tilde{S}^0 \Delta_D^{12*}} \text{---} \xrightarrow{\tilde{D}^0} \text{---} \xrightarrow{\quad} d \\
\downarrow \tilde{g}, \chi_k^0 \\
d \xleftarrow{\quad} \text{---} \xleftarrow{\tilde{D}^0 \Delta_D^{12}} \text{---} \xleftarrow{\tilde{S}^0} \text{---} \xleftarrow{\quad} s
\end{array}
\end{array}
+ \mathcal{O}((\Delta_D^{IJ})^3)$$

Figure 6: Gluino and neutralino contributions to $\bar{K}^0 K^0$ in mass insertion expansion.

Secondly, in a general case with $\Delta^{IJ} \neq 0$, the dependence on particular mass insertions enters into various processes in a correlated way. Correlated vertices are shown in Fig. 7, with $(M_U^2)_{LL} = K(M_D^2)_{LL}K^\dagger$ (see eq. (11)). (However, the right-

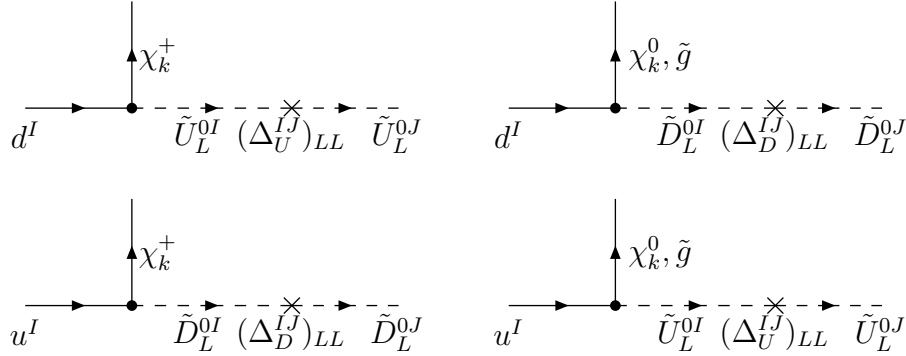


Figure 7: Correlated mass insertion in the left up- and down squark vertices.

handed elements are uncorrelated). These formulae relate, for example, chargino and gluino/neutralino contributions to neutral meson mixing. In addition, the same elements (Δ_{LL} , Δ_{RR} and Δ_{LR}) may enter various processes, e.g. as illustrated in Fig. 8. These correlations have to be taken into account in a complete and systematic study of FCNC transitions in the MSSM.

Having presented the necessary formalism, we proceed to discussing bounds on the sfermion mass matrices obtained from the experimentally observed strong suppression of the FCNC effects.

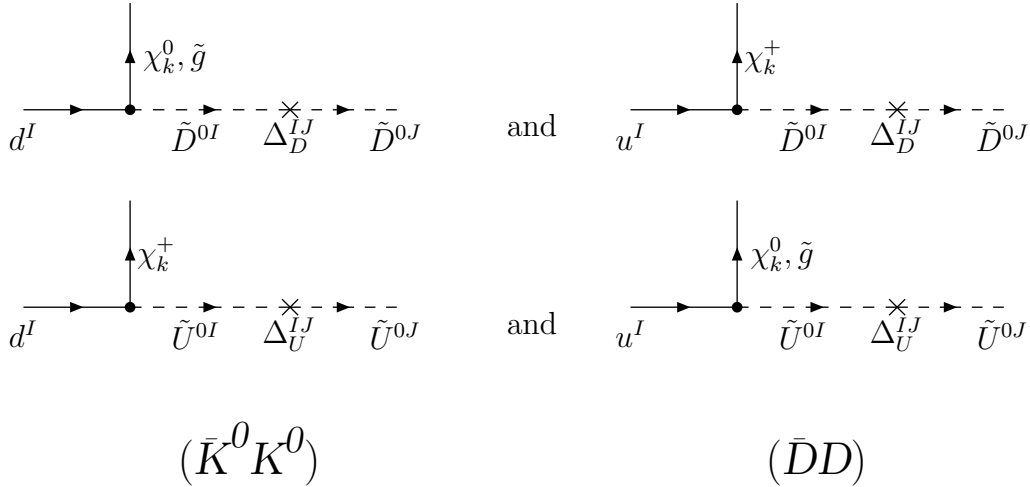


Figure 8: Identical mass insertions in the $\bar{K}^0 K^0$ and $\bar{D}^0 D^0$ mixing.

3 Bounds on sfermion masses from FCNC processes

Strong experimental suppression of the FCNC transitions puts severe upper bounds on various entries in the sfermion mass matrices of eq. (7) at low energy. Such bounds are of crucial interest for the theory (as yet unknown) of soft supersymmetry breaking. As we have already mentioned, a systematic discussion of such bounds should include all potential contributions and correlations among them. However, in the first approximation, one can neglect all but the gluino (photino) exchange contributions to the FCNC transitions in the quark (lepton) sector. Order-of-magnitude bounds on the off-diagonal entries in the squark mass matrices are then obtained under the assumption that these contributions saturate the experimental results [3, 4]. Bounds on splittings between diagonal elements of $(M_{\tilde{U}}^2)_{LL}$ and $(M_{\tilde{D}}^2)_{LL}$ can then be obtained with use of eq. (11). Such bounds have a virtue of being relatively parameter independent.

In the next step, it is also interesting to discuss how these bounds can be modified in a complete analysis, with all contributions and interference between them included. We shall see that cancellations can indeed occur and weaken the limits.

However, large cancellations affecting their order of magnitude would require certain fine-tuning of the MSSM parameters. Thus, we may conclude that the bounds obtained from the gluino (photino) contributions indeed reflect the acceptable structure of the mass matrices, at least up to an order of magnitude.

The most up-to-date set of bounds on the flavour off-diagonal entries in the sfermion mass matrices is given in ref. [4] (for earlier results see [3, 4] and references therein). We shall not repeat details of those analyses here. Very briefly, the bounds on δ_D^{12} , δ_D^{13} and δ_U^{12} are obtained from gluino contributions to the $\bar{K}^0 K^0$, $\bar{B}_d^0 B_d^0$ and $\bar{D}^0 D^0$ mixing, respectively. The contributions are given by box diagrams which are proportional to biproducts of δ 's of different chiralities. The bounds are obtained by assuming that each term of the expansion in the biproducts of δ 's saturates by itself the experimental results.

In the analysis of neutral meson mixing, one usually introduces an effective hamiltonian built out of flavour changing four-quark operators. The operators arising in the SM are built out of left-handed quark fields only. They arise in the MSSM, too. However, the MSSM interactions can generate in addition a whole set of extra operators containing quarks of both chiralities. In the case of SM-like operators, the effect of supersymmetry is seen in a modification of their Wilson coefficients. Matrix elements of these operators between neutral meson states are the same as in the SM. Their values are estimated from lattice calculations and parametrized by quantities denoted by e.g. B_K or B_{B_d} . However, no lattice results are available for the extra operators. One has to rely on rough PCAC estimates only (see refs. [3, 4] for more details). However, this is still a correct approach, so long as only order-of-magnitude bounds on δ^{IJ} are being estimated.

Due to the Appelquist-Carazzone decoupling, bounds on δ^{IJ} become weaker when masses of squarks and gluinos increase. When all the squark masses $m_{\tilde{q}}$ are close in size, we can parametrize this suppression by $m_{max} = \max(m_{\tilde{q}}, m_{\tilde{g}})$. Neutral meson mixing gives us bounds on δ^{IJ}/m_{max} . On the other hand, the limits do not depend strongly on the ratio

$$r_{\tilde{q}\tilde{g}} = \frac{\min(m_{\tilde{q}}, m_{\tilde{g}})}{\max(m_{\tilde{q}}, m_{\tilde{g}})}. \quad (18)$$

Even changing $r_{\tilde{q}\tilde{g}}$ in its whole domain $[0, 1]$ (for both $m_{\tilde{q}} > m_{\tilde{g}}$ and $m_{\tilde{q}} < m_{\tilde{g}}$) results in changing bounds on e.g. $(\delta_D^{12})_{LL}/m_{max}$ by less than an order of magnitude.⁵

For $r_{\tilde{q}\tilde{g}} = 1$ the bounds on flavour changing entries in the squark mass matrices can be summarized as follows:

$$|(\delta_D)_{LL}|, |(\delta_D)_{RR}| \lesssim \left(\begin{array}{c|c|c} & 0.08 \frac{m_{max}}{1 \text{ TeV}} & 0.2 \frac{m_{max}}{1 \text{ TeV}} \\ \hline & & 30 \left(\frac{m_{max}}{1 \text{ TeV}} \right)^2 \\ \hline \end{array} \right), \quad (19)$$

$$|(\delta_D)_{LR}| \lesssim \left(\begin{array}{c|c|c} & 0.009 \frac{m_{max}}{1 \text{ TeV}} & 0.07 \frac{m_{max}}{1 \text{ TeV}} \\ \hline 0.009 \frac{m_{max}}{1 \text{ TeV}} & & 0.03 \frac{m_{max}}{1 \text{ TeV}} \\ \hline 0.07 \frac{m_{max}}{1 \text{ TeV}} & 0.03 \frac{m_{max}}{1 \text{ TeV}} & \end{array} \right), \quad (20)$$

$$|(\delta_U)_{LL}| \lesssim \left(\begin{array}{c|c|c} & 0.2 \frac{m_{max}}{1 \text{ TeV}} & \mathcal{O}(\max[(\delta_D^{13})_{LL}, (\delta_U^{12})_{LL} \frac{K^{13}}{K^{12}}]) \\ \hline & & \mathcal{O}(\max[(\delta_D^{23})_{LL}, (\delta_U^{12})_{LL} \frac{K^{23}}{K^{12}}]) \\ \hline \end{array} \right), \quad (21)$$

$$|(\delta_U)_{RR}| \lesssim \left(\begin{array}{c|c|c} & 0.2 \frac{m_{max}}{1 \text{ TeV}} & ? \\ \hline & & ? \\ \hline \end{array} \right), \quad (22)$$

$$|(\delta_U)_{LR}| \lesssim \left(\begin{array}{c|c|c} & 0.2 \frac{m_{max}}{1 \text{ TeV}} & * \\ \hline 0.2 \frac{m_{max}}{1 \text{ TeV}} & & * \\ \hline ? & ? & \end{array} \right). \quad (23)$$

The off-diagonal entries which can be obtained from hermiticity have been left empty. Question marks denote unconstrained entries which would require experimental information on rare top quark decays. Stars denote the entries which are unconstrained by gluino exchanges but receive bounds from chargino-squark loops (see “note added”). Bounds on the (23) and (32) entries of δ_D matrices were obtained from $b \rightarrow s\gamma$ decay. Estimates for (13) and (23) entries in $(\delta_U)_{LL}$ are found from the relation (11). We discuss consequences of this relation in more detail below.

Limits on leptonic δ_L obtained from $l^I \rightarrow l^J \gamma$ decays are as follows:

$$|(\delta_L)_{LL}|, |(\delta_L)_{RR}| \lesssim \left(\begin{array}{c|c|c} & 0.2 \left(\frac{m_{max}}{500 \text{ GeV}} \right)^2 & 700 \left(\frac{m_{max}}{500 \text{ GeV}} \right)^2 \\ \hline & & 100 \left(\frac{m_{max}}{500 \text{ GeV}} \right)^2 \\ \hline \end{array} \right), \quad (24)$$

$$|(\delta_L)_{LR}| \lesssim \left(\begin{array}{c|c|c} & 1 \times 10^{-5} \frac{m_{max}}{500 \text{ GeV}} & 0.5 \frac{m_{max}}{500 \text{ GeV}} \\ \hline 1 \times 10^{-5} \frac{m_{max}}{500 \text{ GeV}} & & 0.1 \frac{m_{max}}{500 \text{ GeV}} \\ \hline 0.5 \frac{m_{max}}{500 \text{ GeV}} & 0.1 \frac{m_{max}}{500 \text{ GeV}} & \end{array} \right). \quad (25)$$

⁵ This is not true inside a small region $1.4 < m_{\tilde{g}}/m_{\tilde{q}} < 1.7$ where accidental cancellations occur. In this region, there is a point where gluino-squark contributions to neutral meson mixing give no limit on δ_{LL} alone.

In this case, m_{max} stands for $\max(m_{\tilde{l}}, m_{\tilde{\gamma}})$. The presented numerical bounds correspond to equal slepton and photino masses, i.e. to $r_{\tilde{l}\tilde{\gamma}} = 1$. The ratio $r_{\tilde{l}\tilde{\gamma}}$ is defined analogously to eq. (18). The bounds do not depend strongly on this ratio, similarly to the squark-gluino case.

It is important to note that the limits on the δ_{LR} matrices originating from gluino and photino loops are symmetric not because the matrices themselves are symmetric, but because the considered amplitudes depend on their off-diagonal entries in a symmetric manner. Furthermore, we have to mention that we have identified absolute values of all the entries with their real parts. This is reasonable, because CP-violating phenomena put bounds on the imaginary parts which are usually much stronger than bounds on real parts. In ref. [4], one can find explicit bounds on the imaginary parts of δ_U , δ_D and δ_L .

The method applied for finding bounds on $|\delta_U|$ and $|\delta_D|$ gives us “independent” limits on certain products of these entries. too. For instance

$$\begin{aligned} \sqrt{|(\delta_D^{12})_{LL}(\delta_D^{12})_{RR}|} &\lesssim 0.006 \frac{m_{max}}{1 \text{ TeV}} \\ \sqrt{|(\delta_D^{13})_{LL}(\delta_D^{13})_{RR}|} &\lesssim 0.04 \frac{m_{max}}{1 \text{ TeV}} \\ \sqrt{|(\delta_U^{12})_{LL}(\delta_U^{12})_{RR}|} &\lesssim 0.04 \frac{m_{max}}{1 \text{ TeV}}. \end{aligned} \tag{26}$$

These bounds look more restrictive than the previously given bounds on δ_{LL}^{IJ} and δ_{RR}^{IJ} separately. Actually, the allowed region in the $Re(\delta_{LL}^{IJ})-Re(\delta_{RR}^{IJ})$ plane (for given (IJ)) is bounded by two hyperbolae centered at the origin. The symmetry axes of these hyperbolae are close to being horizontal or vertical. This is why the product of the two δ 's is more restricted than each δ alone. No strict bound on δ 's exists when fine-tuning between them is allowed. Barring fine-tuning, one can only conclude that the expected sizes of δ 's are somewhere between those in eq. (26) and those in eqs. (19) and (21).

It is interesting to notice, that box diagrams constrain δ/m_{max} , while the penguin ones give bounds on δ/m_{max}^2 . An exception from the latter rule are bounds on $(\delta^{IJ})_{LR}$ from processes receiving important contributions from dimension 5 effective

operators.⁶ Such processes (like $b \rightarrow s\gamma$) give us bounds on $(\delta^{IJ})_{LR}/m_{max}$. Since the limits on squark mass matrices we have listed above originate from box diagrams and from $b \rightarrow s\gamma$, only one of these constraints scales like m_{max}^2 .

The limits we have discussed so far (following ref. [4]) are derived from gluino and photino exchange contributions to various FCNC processes. It is also interesting to consider bounds originating from diagrams with chargino exchanges. As an example, chargino–(up squark) contribution to $b \rightarrow s\gamma$ decay is discussed in more detail in Appendix A. As seen in Appendix A, chargino diagrams restrict certain linear combinations of diagonal mass splittings and off-diagonal elements of $(M_U^2)_{LL}$ (at the leading order in these quantities). Those linear combinations turn out to be equal to the off-diagonal elements of $(M_D^2)_{LL}$ only. The relation (11) is essential for making this observation.

We argue in Appendix A that the same conclusion holds for other processes: Chargino, neutralino and gluino contributions to processes involving down quarks in the initial and final states (e.g. $b \rightarrow s\gamma$ decay, $\bar{K}^0 K^0$ and $\bar{B}_d^0 B_d^0$ mixing) are all directly sensitive to the structure of $(M_D^2)_{LL}$, not $(M_U^2)_{LL}$. Similarly, processes involving up quarks in the initial and final states (like $\bar{D}^0 D^0$ mixing) are directly sensitive to the structure of $(M_U^2)_{LL}$. The constraints on $(\delta_{U,D})_{LL}$ from chargino loops are expected to be of the same order of magnitude as the gluino ones.⁷ On the other hand, bounds from chargino loops on $(\delta_{U,D})_{LR}$ and $(\delta_{U,D})_{RR}$ (except for $(\delta_U^{13})_{LR}$ and $(\delta_U^{23})_{LR}$) are inefficient due to small Yukawa couplings of the first two generations.

Let us now turn to restrictions on diagonal entries of the matrices $(M_U^2)_{LL}$ and $(M_D^2)_{LL}$. Using again eq. (11), we can express splitting between these diagonal entries in terms of the off-diagonal ones. The exact formulae are the following:

$$(m_{UI}^2)_{LL} - (m_{UJ}^2)_{LL} = \frac{1}{K_{IJ}} [K(\Delta_D)_{LL} - (\Delta_U)_{LL}K]^{IJ} - \frac{1}{K_{JJ}} [K(\Delta_D)_{LL} - (\Delta_U)_{LL}K]^{JJ}, \quad (27)$$

⁶ All such operators can be reduced by equations of motion to the so-called “magnetic moment” operators, like the two we give later in eqs. (45) and (46).

⁷ Suppression by electroweak coupling is off-set by relatively smaller chargino mass, at least when GUT relations between gaugino masses are assumed.

$$(m_{DI}^2)_{LL} - (m_{DJ}^2)_{LL} = \frac{1}{K^{IJ}}[K(\Delta_D)_{LL} - (\Delta_U)_{LL}K]^{IJ} - \frac{1}{K^{II}}[K(\Delta_D)_{LL} - (\Delta_U)_{LL}K]^{II}, \quad (28)$$

where no summation over the indices I and J is understood.⁸ Our previous discussion implies that eqs. (27) and (28) are the only available source of information concerning diagonal mass splittings in $(M_U^2)_{LL}$ and $(M_D^2)_{LL}$, up to $\mathcal{O}((\delta m^2/m^2)^2)$ effects.

The presence of $1/K^{IJ}$ in the constraints on mass splitting in eqs. (27) and (28) makes these bounds completely inefficient for the third generation of squarks. Even the bound on the splitting between the first two generations is rather weak when bounds on δ 's from gluino exchanges are used. Approximately, it reads

$$\frac{|(m_{U1}^2)_{LL} - (m_{U2}^2)_{LL}|}{m_{\tilde{q}}^2}, \frac{|(m_{D1}^2)_{LL} - (m_{D2}^2)_{LL}|}{m_{\tilde{q}}^2} \lesssim \frac{|(\delta_U^{12})_{LL}| + |(\delta_D^{12})_{LL}|}{K^{12}} \simeq 1 \times \frac{m_{max}}{1 \text{ TeV}} \quad (29)$$

This bound could become a factor of two lower if the experimental constraints on $\bar{D}^0 D^0$ mixing improved by the same factor. Furthermore, nonvanishing δ_{RR} would improve it (indirectly) as well, because of correlations between δ_{LL} and δ_{RR} (see eq. (26) and below). However, one should keep in mind that all the bounds we discuss here are only order-of-magnitude ones.

We have already mentioned that chargino loops give us direct constraints only on the off-diagonal elements of $(M_U^2)_{LL}$ and $(M_D^2)_{LL}$. Consequently, bounds from chargino diagrams on diagonal mass splittings in these matrices can be derived from eqs. (27) and (28) only. They are similar to those given in eq. (29). On the other hand, direct bounds from chargino diagrams on diagonal mass splittings in the left-right and right-right blocks of squark mass matrices are inefficient due to small Yukawa couplings of the first two generations. This is because winos couple to left-handed quarks only while higgsino couplings to the first two generations are very small.

Another way of restricting the off-diagonal elements and diagonal mass splittings

⁸ A relation between Δ_U and Δ_D which is independent of the diagonal entries can be obtained e.g. from the first equation by adding its $(IJ) = (12), (23)$ and (31) components. This is where the estimates for $(\delta_U^{13})_{LL}$ and $(\delta_U^{23})_{LL}$ in eq. (21) originate from.

in the squark mass matrices is to require that supersymmetric contributions to FCNC processes do not exceed the Standard Model ones. This allows to see more easily the relation between squark mass splittings and the GIM mechanism in the SM. As an example, let us consider this part of the gluino contribution to Δm_K which is proportional to $(\delta_D^{12})_{LL}$. Requiring that it is not larger than the (QCD-uncorrected) short-distance SM contribution, we find for $r_{\tilde{q}\tilde{g}} = 1$

$$|(\delta_D^{12})_{LL}| \lesssim \sqrt{\frac{27}{2}} \frac{\alpha_2}{\alpha_3} K^{12} \frac{m_c m_{\tilde{q}}}{M_W^2}, \quad (30)$$

which agrees (within a factor of 2) with the bound quoted in eq. (19). As usual, we have neglected the imaginary part of $(\delta_D^{12})_{LL}$. Inserting the above bound into eq. (29), one finds

$$|m_{\tilde{q}1} - m_{\tilde{q}2}| \lesssim 2\sqrt{\frac{27}{2}} \frac{\alpha_2}{\alpha_3} m_c \frac{m_{\tilde{q}}^2}{M_W^2} \simeq 2m_c \frac{m_{\tilde{q}}^2}{M_W^2} + \mathcal{O}((\delta_U^{12})_{LL}) \quad (31)$$

for both up and down squarks. Thus, if masses of squarks and gluinos were close to M_W and $(\delta_U^{12})_{LL}$ was negligibly small, then differences between masses of left squarks of the first two generations would need to be close to the charm quark mass (or smaller). This would mean degeneracy by at most a few percent. On the other hand, if masses of squarks and gluinos were close to 1 TeV (but $(\delta_U^{12})_{LL}$ was still negligible), the first two left squark generations could differ in mass by even 50%. These restrictions get weaker by about a factor of 2 to 3 when we take into account nonvanishing $(\delta_U^{12})_{LL}$ within the bounds allowed by $\bar{D}^0 D^0$ mixing data (eq. (21)).

Bounds on off-diagonal elements and diagonal mass splittings in the squark mass matrices are sensitive to interference between chargino and gluino contributions. Sizable effects in bounds derived from neutral meson mixing may be observed mainly when the limits on $(\delta_{U,D})_{LL}$ are considered. In the LR and RR cases, chargino contributions are suppressed by small Yukawa couplings whenever both gluinos and charginos contribute proportionally to the same δ . In Figs. 9,10 we present an example of bounds on $(\delta_D^{12})_{LL}$ following from the ϵ_K measurement for a chosen set of SUSY parameters and KM phase: $\tan \beta = 1.8$, $m_{\tilde{\chi}_1^\pm} = m_{\tilde{T}_R} = 100$ GeV, $m_{gluino} = m_{\tilde{T}_L} = 500$ GeV, $m_{H^\pm} = 1000$ GeV, $\theta_{LR} = 0$, $\sin \delta^{KM} = 0.7$. In Fig. 9, we plot values

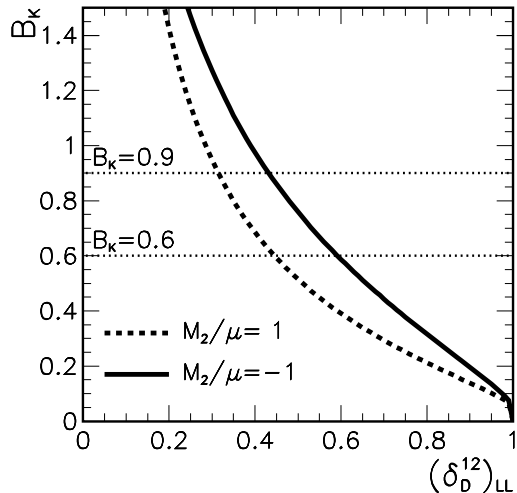


Figure 9: Values of B_K necessary to restore the experimental result for ϵ_K as a function of $(\delta_D^{12})_{LL}$ for a chosen set of SUSY parameters (see the text).

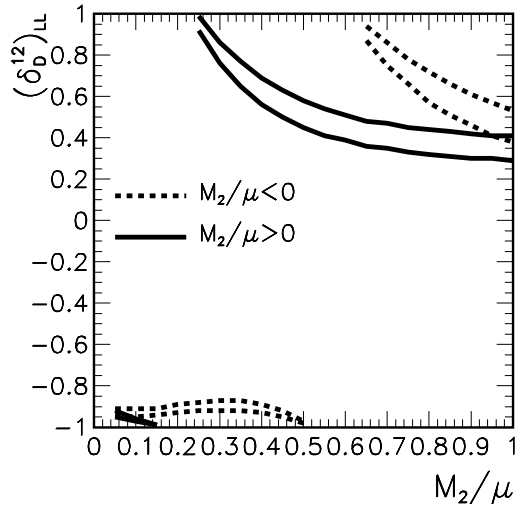


Figure 10: Upper and lower bounds on $(\delta_D^{12})_{LL}$ as a function of M_2/μ for a chosen set of SUSY parameters (see the text).

of the hadronic matrix element parameter B_K necessary to restore the experimental result $\epsilon_K = (2.26 \pm 0.02) 10^{-3}$ for given value of $(\delta_D^{12})_{LL}$ and compare them with theoretical estimates $0.6 \leq B_K \leq 0.9$ [5]. Acceptable range for B_K is denoted by dotted horizontal lines which determine the bounds on $(\delta_D^{12})_{LL}$. As can be seen from Fig. 9, detailed limits on $(\delta_D^{12})_{LL}$ depend on the chargino mixing angles determined by M_2/μ . An example of such a dependence is shown in Fig 10. Bounds on $(\delta_D^{12})_{LL}$ obtained from the condition (see eq. (34) in the next section):

$$0.6 \leq B_K((\delta_D^{12})_{LL}) = \frac{\epsilon_K^{exp}}{\epsilon_K^{theor}(B_K = 1, (\delta_D^{12})_{LL})} \leq 0.9 \quad (32)$$

are plotted there as a function of M_2/μ . We see that when cancellations between the chargino and gluino contributions occur, the bounds on $(\delta_D^{12})_{LL}$ can be weaker even by an order of magnitude (or more). For some values of M_2/μ in fig. 10, chargino and gluino contributions cancel exactly, and bounds on $(\delta_D^{12})_{LL}$ disappear completely. Thus, if we are ready to accept some degree of fine-tuning, the bounds on $(\delta_{U,D}^{IJ})_{LL}$ can be significantly weaker than those given in matrices (19,21). However,

we should stress that there is no similar mechanism for weakening the bounds on $(\delta_{U,D}^{IJ})_{LR}$, $(\delta_{U,D}^{IJ})_{RR}$. Therefore, it is clear from eq. (26) that the overall weakening of the bounds given in (19,21) can only be moderate. We may conclude again that (19,21) reflect the expected order of magnitude of bounds on δ 's, even in the presence of some fine-tuning.

In the end of this section, let us make a comment about FCNC processes other than $b \rightarrow s\gamma$ and neutral meson mixing. As far as processes involving down quarks in the initial and final states are considered, one can expect that bounds roughly similar to those in eqs. (19)–(23) can be derived by requiring that SUSY amplitudes do not exceed SM ones. However, experimental constraints on FCNC processes other than $\bar{K}^0 K^0$ and $\bar{B}^0 B^0$ mixing as well as $b \rightarrow s\gamma$ are usually well above the (short-distance) SM predictions. This is why $b \rightarrow s\gamma$ and neutral meson mixing are most restrictive for most SUSY parameter choices.

Nevertheless, other processes can be helpful in some limited domains of the MSSM parameter space. For instance, large SUSY contributions to $b \rightarrow s$ *gluon* can be sometimes obtained without violating $b \rightarrow s\gamma$ bounds [6]. Certain asymmetries in $b \rightarrow se^+e^-$ are essential to determine the sign of $b \rightarrow s\gamma$ amplitude [7, 8], which matters in studying the allowed MSSM parameter space. Last but not least, various CP-violating observables like ϵ'/ϵ , electric dipole moments or $K_L \rightarrow \pi^0\nu\bar{\nu}$ decay rate are essential in verifying whether other than KM phase sources of CP violation occur in the MSSM [9].

As far as FCNC processes involving up quarks are considered, improving experimental bounds on $\bar{D}^0 D^0$ mixing seems more promising than studying processes like $c \rightarrow u\gamma$. Mixing with the third generation can be restricted only when rare top quark decays become experimentally accessible. Before this happens, some of the superpartners may be already discovered.

4 FCNC with light superpartners.

The bounds discussed in section 3 must be satisfied in any realistic supersymmetric extension of the SM. It should be stressed that there are two general ways of

achieving this. The most straightforward solution occurs (see e.g. ref. [10]) when sfermions of the first two generations are sufficiently heavy, so that new contributions to the FCNC processes in (1,2) sector decouple by the Appelquist-Carrazone theorem [11]. Indeed, the strongest bounds are for (1,2) sector. Satisfying them for $\delta^{12} \sim \mathcal{O}(1)$ requires quite large masses of the first two generations of sfermions $m_{1,2} \sim \mathcal{O}(10 \text{ TeV})$. On the other hand, the constraints in the (1,3) and (2,3) sector are much weaker and satisfying them with $m_3 \sim \mathcal{O}(M_Z)$, i.e. $\sqrt{m_3 m_{1,2}} \sim \mathcal{O}(1 \text{ TeV})$ is easier. As we discuss in the last section, this possibility is not at all unnatural, and does not ruin the virtues of supersymmetry as a solution to the hierarchy problem.

Another possibility is that for some deeper theoretical reasons⁹ all the δ^{IJ} ($I, J = 1..3$) are indeed very small at low energies. In addition, if high degeneracy of the first two sfermion generations occurs, their masses are bounded from below only by the present direct search limits. These limits are close to 200 GeV at present [12].

It is interesting to observe that both solutions allow for light third generation of sfermions. Moreover, in the limit when both solutions are “perfect” and assure negligible contributions from the squark flavour mixing, the only potentially significant contribution to FCNC transitions may come from the (charged Higgs)-top and chargino-stop loops with Yukawa couplings and KM angles in the vertices.¹⁰ Since, in addition, several arguments (see section 5) suggest that charginos and 3rd generation of sfermions may be among the lightest superpartners, it is interesting to discuss in more detail their impact on FCNC transitions.

The present section is devoted to discussing such a scenario. In the first step, the only extra MSSM contributions to the FCNC processes we consider are the (charged Higgs)-top and chargino-stop loops. Our results depend then on the following parameters (apart from the SM ones):

(i) $\tan \beta$

(ii) Physical masses of the lighter and heavier stop ($m_{\tilde{T}_1}$ and $m_{\tilde{T}_2}$, respectively),

⁹ Some speculative ideas are collected in section 5.

¹⁰ Chargino-sbottom loops could be important in $\bar{D}^0 D^0$ mixing as well. We will not discuss this possibility here, although it could be well motivated in large $\tan \beta$ scenarios.

as well as their mixing angle θ_{LR} . The sign convention for this angle is fixed by requiring that $(Z_U)^{63} \simeq \sin \theta_{LR}$.

- (iii) Chargino mass and mixing parameters. We choose the lightest chargino mass $m_{\chi_1^\pm}$ and the ratio M_2/μ as input parameters.
- (iv) The charged Higgs boson mass m_{H^\pm} .

In most of the numerical examples, we will decouple the heavier stop and assume that the lighter one is dominantly right, i.e. that θ_{LR} is relatively small (of order 10°). This is motivated by studies of supersymmetric effects in electroweak precision observables [13, 14].

In the considered MSSM scenario, various FCNC processes exhibit different sensitivity to supersymmetry. While sizable effects can still occur in the neutral meson mixing ($\bar{K}^0 K^0$ and $\bar{B}^0 B^0$), supersymmetric contributions to other FCNC processes are usually either small or screened by long-distance QCD effects. An exception is the inclusive weak radiative B meson decay $B \rightarrow X_s \gamma$, to which light superpartners can contribute significantly, and where strong interaction effects are under control. In the following, we shall first focus on neutral meson mixing and then discuss the $B \rightarrow X_s \gamma$ decay.

In the considered approach to the MSSM, the results for Δm_{B_d} and ϵ_K read

$$\Delta m_{B_d} = \eta_{QCD} \frac{\alpha_{em}^2 m_t^2}{12 \sin^4 \theta_W M_W^4} f_{B_d}^2 B_{B_d} m_{B_d} |K_{tb} K_{td}^*|^2 |\Delta|, \quad (33)$$

$$|\epsilon_K| = \frac{\sqrt{2} \alpha_{em}^2 m_c^2}{48 \sin^4 \theta_W M_W^4} f_K^2 B_K \frac{m_K}{\Delta m_K} |\mathcal{I} m \Omega|, \quad (34)$$

where

$$\Omega = \eta_{cc} (K_{cs} K_{cd}^*)^2 + 2\eta_{ct} (K_{cs} K_{cd}^* K_{ts} K_{td}^*) f \left(\frac{m_c^2}{M_W^2}, \frac{m_t^2}{M_W^2} \right) + \eta_{tt} (K_{ts} K_{td}^*)^2 \frac{m_t^2}{m_c^2} \Delta, \quad (35)$$

and

$$f(x, y) = \log \frac{y}{x} + \frac{3y}{4(y-1)} \left(1 - \frac{y}{y-1} \log y \right).$$

The charged Higgs and the chargino boxes enter, together with the SM terms, only into the quantity Δ in the above equations. The QCD correction factors η_{cc} , η_{ct} , η_{tt} and η_{QCD} are known up to the next-to-leading accuracy [15].

The KM elements appearing in eqs. (33-35) can be conveniently expressed in terms of the Wolfenstein parameters λ , A , ρ and η [16]

$$K \approx \begin{pmatrix} 1 - \frac{\lambda^2}{2} & \lambda & A\lambda^3(\rho - i\eta) \\ -\lambda - iA^2\lambda^5\eta & 1 - \frac{\lambda^2}{2} + i\mathcal{O}(\lambda^6) & A\lambda^2 \\ A\lambda^3(1 - \rho - i\eta) & -A\lambda^2 - iA\lambda^4\eta & 1 \end{pmatrix} + \mathcal{O}(\lambda^4), \quad (36)$$

where $\lambda = 0.22$ is known from semileptonic kaon and hyperon decays. The leading in λ imaginary parts of all the entries are shown, because most of them are relevant in analyzing CP-violation.

Both in the SM and MSSM, the theoretical predictions for ϵ_K and Δm_{B_d} have some uncertainty due to non-perturbative parameters B_K , $f_{B_d}^2 B_{B_d}$ which are known from lattice calculations, but not very precisely. Moreover, the KM element $K_{td} = A\lambda^3(1 - \rho - i\eta)$ which appears in eqs. (33-35) is not directly measured. Its SM value fitted to the observables in eqs. (33-34) can change after inclusion of new contributions. Thus, the correct approach is to fit the parameters A , ρ , η and Δ in a model independent way to the experimental values of ϵ_K and Δm_{B_d} [17]. The quantities $|K_{cb}|$ and $|K_{ub}/K_{cb}|$ are known from tree level processes. They are practically unaffected by new physics which contributes only at one and more loops.

Here, we give the results of such a fit, with B_K and $f_{B_d}^2 B_{B_d}$ varied in a the following ranges: [5].

$$0.6 < B_K < 0.9 \quad (37)$$

$$0.160 \text{ GeV} < \sqrt{f_{B_d}^2 B_{B_d}} < 0.240 \text{ GeV} \quad (38)$$

In our fit, we use the following experimental results [5, 12]:

$$|K_{cb}| = 0.039 \pm 0.002 \quad (39)$$

$$|K_{ub}/K_{cb}| = 0.08 \pm 0.02 \quad (40)$$

$$|\epsilon_K| = (2.26 \pm 0.02) 10^{-3} \quad (41)$$

$$\Delta m_{B_d} = (3.01 \pm 0.13) 10^{-13} \text{ GeV} \quad (42)$$

In Fig. 11, we show values¹¹ of the parameter Δ obtained from the χ^2 fit of the

¹¹ Here, we assume that Δ is real. This is true in the SM and, to a very good approximation, in the considered approach to the MSSM. However, in a general MSSM, Δ could develop a sizable imaginary part.

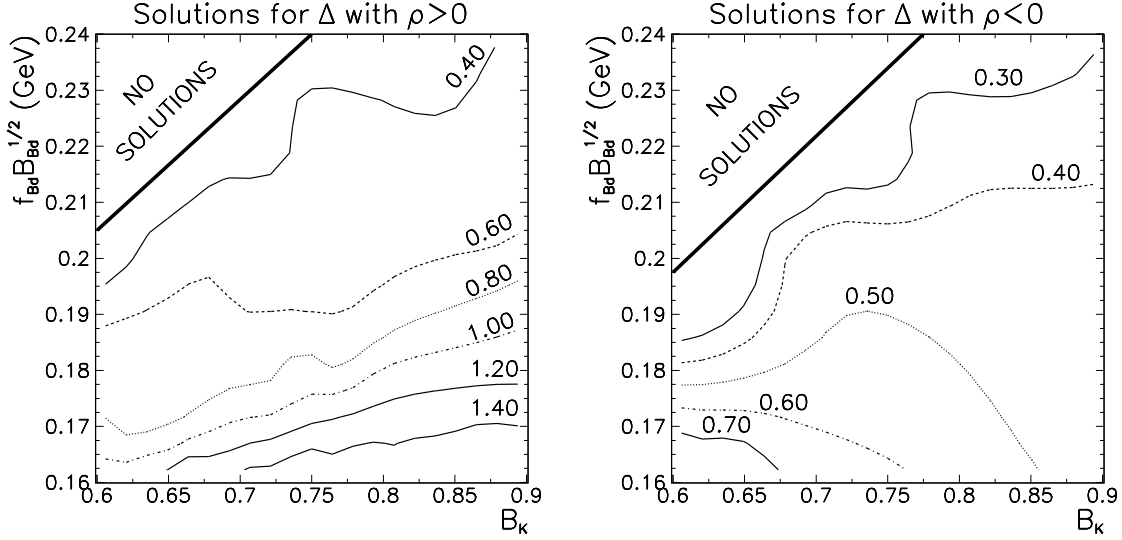


Figure 11: Contour lines of the parameter Δ minimizing the χ^2 fit to experimentally measured values of $|K_{cb}|$, $|K_{ub}/K_{cb}|$, ϵ_K and Δm_{B_d} .

parameters (A, ρ, η, Δ) to the four quantities listed in eqs. (39-42), as a function of B_K and $f_{B_d}(B_{B_d})^{1/2}$. The left and right plots in Fig. 11 are equivalent to two different solutions for χ^2 minimum with the Wolfenstein parameter $\rho > 0$ and $\rho < 0$, respectively. In our fit, we require $\chi_{min}^2 \leq 4$. As can be seen from both plots of Fig. 11, no such solutions exist for small B_K and large $f_{B_d}(B_{B_d})^{1/2}$, where χ_{min}^2 starts to grow quickly. In the remaining $(B_K, f_{B_d}(B_{B_d})^{1/2})$ range, χ_{min}^2 is close or equal to 0, excluding only those values of $(B_K, f_{B_d}(B_{B_d})^{1/2})$ which are very close to the thick boundary line marked in both plots. The contour lines show values of Δ which exactly minimize the χ^2 fit. The 1σ errors on Δ obtained from the fit are typically of the order of $\mathcal{O}(0.1 - 0.2)$, depending on the specific values of B_K and $f_{B_d}(B_{B_d})^{1/2}$. Results plotted in Fig. 11 can be compared with the theoretical prediction for the parameter Δ in the SM: $\Delta_{SM} \approx 0.53$. As can be seen from Fig. 11, larger values of $\Delta > \Delta_{SM}$ (interesting in the MSSM, as discussed later) prefer $\rho > 0$, small values of $f_{B_d}(B_{B_d})^{1/2}$ and, to a lesser extent, large B_K . For instance, $\Delta > 1$ requires $\rho > 0$ and $f_{B_d}(B_{B_d})^{1/2} < 0.19$ GeV. Scanning over allowed range for B_K and $f_{B_d}(B_{B_d})^{1/2}$, defined in eqs. (37-38), gives the “absolute” bounds on Δ . Such bounds are not very

tight. After including 1σ errors on Δ , they are roughly

$$0.2 \lesssim \Delta \lesssim 2.0 \quad (43)$$

In Fig. 12, we plot the allowed ranges of ρ and η for several fixed values of $\Delta =$

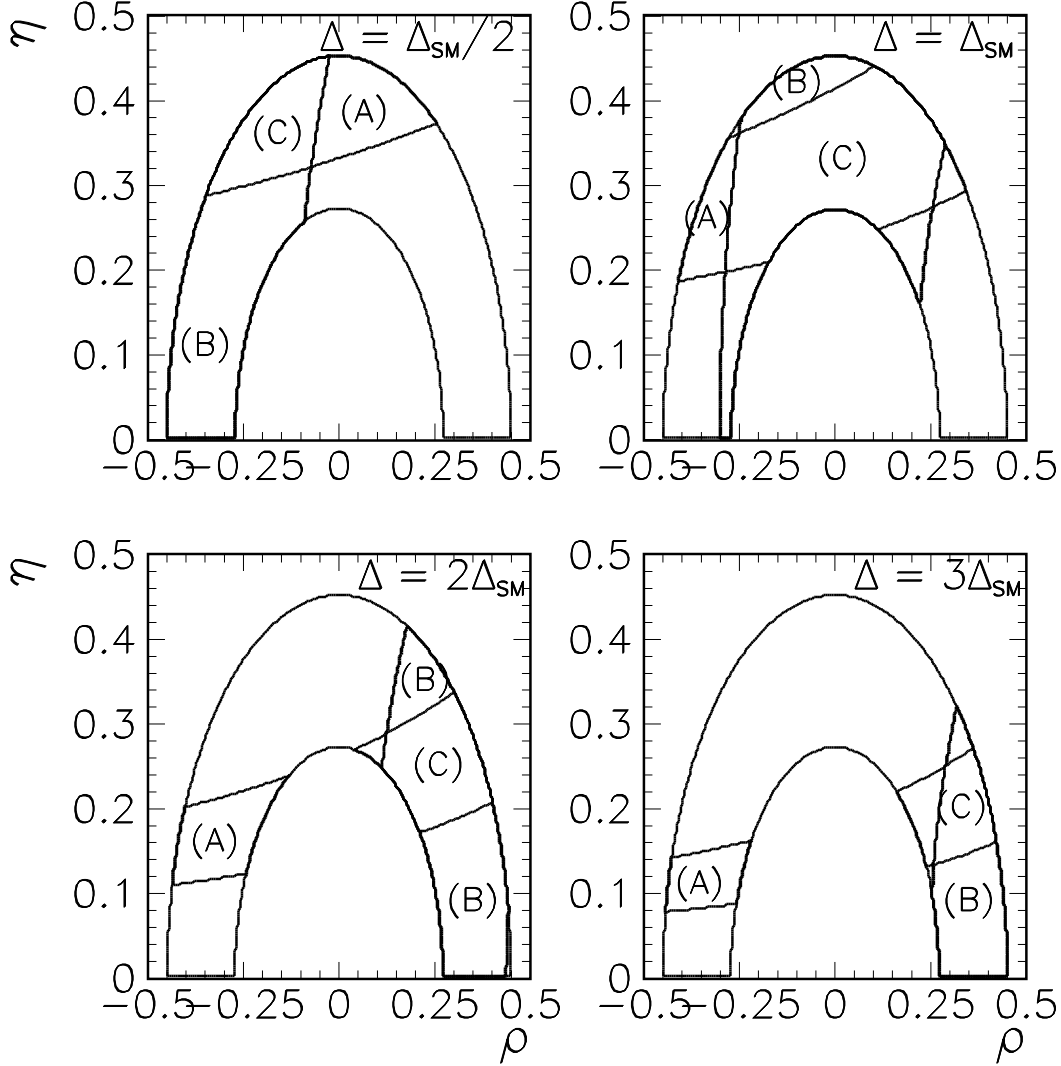


Figure 12: Allowed regions in the (ρ, η) plane for four values of Δ : (A) - allowed by ϵ_K , (B) - allowed by Δm_{B_d} , (C) - allowed by ϵ_K and Δm_{B_d} . The value of Δ_{SM} is approximately equal to 0.53.

$\frac{1}{2}\Delta_{SM}, \Delta_{SM}, 2\Delta_{SM}, 3\Delta_{SM}$ and changing $B_K, f_{B_d}(B_{B_d})^{1/2}$ in the ranges specified in eqs. (37-38). The allowed half-ring visible in the plots of Fig. 12 originates from

$|K_{ub}/K_{cb}|$ given in eq. (40). The measurement of Δm_{B_d} allows another ring in the (ρ, η) plane. It is centered at $(\rho, \eta) = (1, 0)$. Its interesting part is approximately parallel to the η axis. It moves to the right (towards larger ρ) when Δ increases. The range bounded by ϵ_K is approximately parallel to the ρ axis. It moves down (towards smaller η) with increasing Δ . Taking both effects into account, we can see that small Δ prefers negative ρ and large η , $\Delta \sim \Delta_{SM}$ gives the biggest allowed range for ρ and η with both $\rho < 0$ and $\rho > 0$ possible, whereas larger $\Delta \geq 1$ requires positive ρ and smaller η .

In the next step, we correlate the value of Δ with masses and mixings in the MSSM. In Fig. 13, we plot contour lines of constant Δ for light SUSY spectrum, i.e. in the range where SUSY effects are most visible. As seen from Fig. 13, the values of Δ in the MSSM are always bigger than in the SM, i.e. the new contributions to Δ from the Higgs and chargino sectors have the same sign as $\Delta_{SM} \approx 0.53$. This is a general conclusion, always true for the Higgs contribution and valid also for the chargino-stop contribution when SUSY parameters are chosen as in this section. The actual value of the supersymmetric contribution to Δ depends strongly on the ratio M_2/μ . The charged Higgs contribution does not depend on this ratio, and increases Δ by about 0.12 for $m_{H^\pm} = 100$ GeV and $\tan\beta = 1.8$, as used in Fig. 13. For small values of $|M_2/\mu|$, when the lighter chargino is predominantly gaugino, the $\chi^- - \tilde{T}_1$ contribution to Δ is very small (of order 10^{-2}) and weakly dependent on the lighter stop mass. This can be easily understood: In this case, the lighter stop is coupled to the lighter chargino mostly through the LR mixing in the stop sector, and the appropriate contribution is suppressed by $\sin^4\theta_{LR}$. For larger values of $|M_2/\mu| \sim 1$, this contribution is bigger and, due to the interference between the diagrams with and without the LR mixing, may reach its maximal value for $\theta_{LR} \neq 0$, depending on the sign of μ . Chargino-lighter stop contributions increase further with $|M_2/\mu|$, when lighter chargino consists predominantly of Higgsino, and become again independent on the sign of μ . In this case, contributions proportional to $Z_U^{63} \approx \sin\theta_{LR}$ are negligible, and varying of θ_{LR} is visible in Δ only via $Z_U^{66} \simeq \cos\theta_{LR}$.

Increasing the charged Higgs mass to $m_{H^\pm} \approx 500$ GeV and chargino mass to

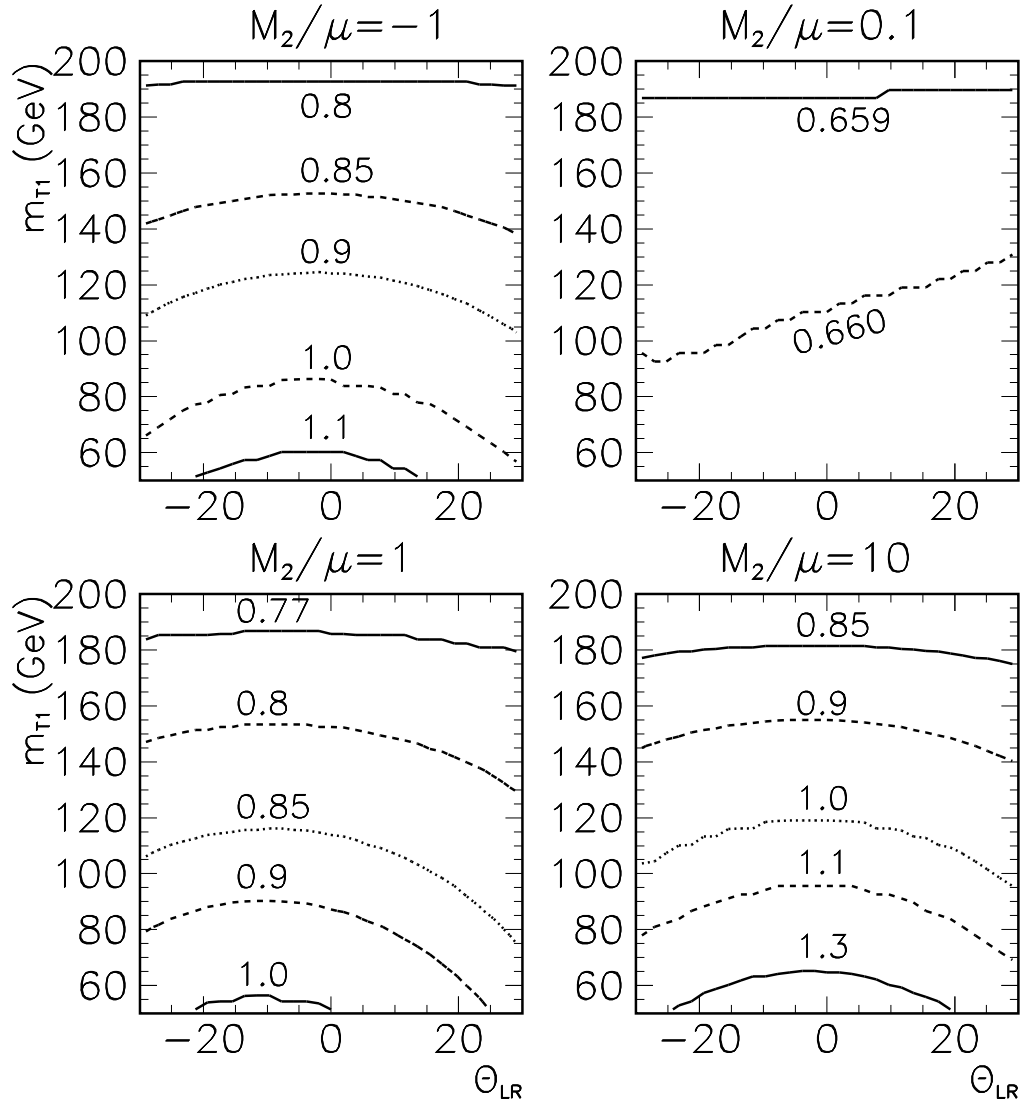


Figure 13: Contour lines of Δ as a function of right stop mass and stop mixing angle for $\tan\beta = 1.8$, $M_{H^+} = 100$ GeV, $M_{\tilde{t}_2} = 250$ GeV, $m_{\chi^-} = 90$ GeV and four chosen M_2/μ ratio values.

$m_{\tilde{\chi}_1^\pm} = 300$ GeV suppresses the magnitude of each contribution by a factor of 3 approximately, but does not change the character of its dependence on θ_{LR} . The results illustrated in Fig. 13 are also weakly dependent on the mass of the left stop: Increasing $M_{\tilde{T}_2}$ from 250 to 500 GeV modifies Δ only marginally.

We now turn to the discussion of $B \rightarrow X_s \gamma$. Sample SM and MSSM diagrams for the $b \rightarrow s \gamma$ transition are shown in Figs. 14 and 15, respectively

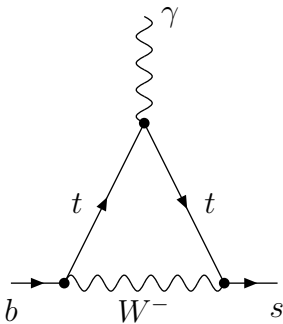


Figure 14: Sample SM diagram.

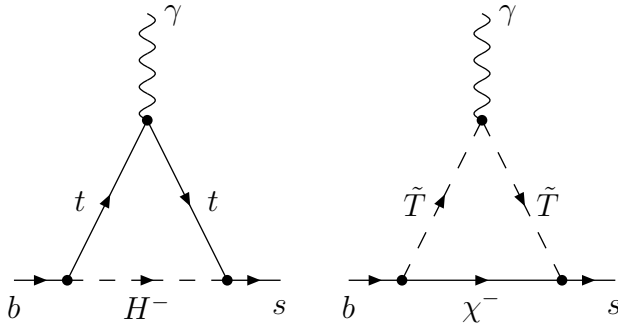


Figure 15: Sample MSSM diagrams.

Dressing these diagrams with one or more gluons gives us QCD contributions enhanced by large logarithms $\ln(M_W^2/m_b^2)$. In the SM, they increase the decay rate by more than a factor of 2. Resumming these large QCD logarithms up to next-to-leading order (NLO) is necessary to acquire sufficient accuracy [18]. Such a resummation has been recently accomplished in the SM [19, 20, 21, 22].

The analysis of $B \rightarrow X_s \gamma$ decay begins with introducing an effective Hamiltonian

$$H_{eff} = -\frac{4G_F}{\sqrt{2}} K_{ts}^* K_{tb} \sum_{i=1}^8 C_i(\mu) P_i(\mu) \quad (44)$$

where P_i are the relevant operators and $C_i(\mu)$ are their Wilson coefficients. Here, we need to give only two of these operators explicitly

$$P_7 = \frac{e}{16\pi^2} m_b (\bar{s}_L \sigma^{\mu\nu} b_R) F_{\mu\nu} \quad (45)$$

$$P_8 = \frac{g_3}{16\pi^2} m_b (\bar{s}_L \sigma^{\mu\nu} T^a b_R) G_{\mu\nu}^a \quad (46)$$

where $F_{\mu\nu}$ and $G_{\mu\nu}^a$ are the photonic and gluonic field strength tensors, respectively. Resummation of large logarithms $\ln(M_W^2/m_b^2)$ is achieved by evolving the coefficients

$C_i(\mu)$ from $\mu \sim M_W$ to $\mu \sim m_b$ according to the renormalization group equations. Feynman rules derived from the effective Hamiltonian are then used to calculate the b -quark decay rate $\Gamma[b \rightarrow X_s \gamma]$ which is a good approximation to the corresponding B -meson decay rate [23, 24]. All these calculations are identical in the SM and MSSM (also at NLO), except for that the initial numerical values of the Wilson coefficients C_7 and C_8 at $\mu \sim M_W$ are different¹². The leading-order MSSM contributions to $C_7(M_W)$ and $C_8(M_W)$ are well known [25, 8]. Here, we quote only the SM, charged higgs and chargino contributions to $C_7(M_W)$

$$C_7^{(0)SM}(M_W) = \frac{1}{4} \frac{m_t^2}{M_W^2} f_1 \left(\frac{m_t^2}{M_W^2} \right) \quad (47)$$

$$C_7^{(0)H^\pm}(M_W) = \frac{1}{12} \frac{m_t^2}{M_{H^\pm}^2} \cot^2 \beta f_1 \left(\frac{m_t^2}{M_{H^\pm}^2} \right) + \frac{1}{6} f_2 \left(\frac{m_t^2}{M_{H^\pm}^2} \right) \quad (48)$$

$$C_7^{(0)\chi^\pm}(M_W) = \frac{1}{K_{ts}^* K_{tb}} \sum_{i=1}^6 \sum_{p=1}^2 \frac{M_W^2}{m_{\chi_p^\pm}^2} \left\{ -\frac{1}{6} A_{i2}^{p*} A_{i3}^p f_1 \left(\frac{m_{\tilde{U}_i}^2}{m_{\chi_p^\pm}^2} \right) + \frac{1}{3} A_{i2}^{p*} B_{i3}^p \frac{m_{\chi_p^\pm}}{m_b} f_2 \left(\frac{m_{\tilde{U}_i}^2}{m_{\chi_p^\pm}^2} \right) \right\} \quad (49)$$

where

$$f_1(x) = \frac{3x^2 - 2x}{(1-x)^4} \log x + \frac{8x^2 + 5x - 7}{6(1-x)^3},$$

$$f_2(x) = \frac{-3x^2 + 2x}{(1-x)^3} \log x + \frac{-5x^2 + 3x}{2(1-x)^2}.$$

The matrices A and B originate from the vertices in Fig. 1

$$A_{kJ}^p = \left[-Z_U^{Ik*} Z_{1p}^+ + \frac{1}{\sqrt{2} M_W \sin \beta} m_u^{II} Z_U^{(I+3)k*} Z_{2p}^+ \right] K^{IJ},$$

$$B_{kJ}^p = \frac{1}{\sqrt{2} M_W \cos \beta} Z_U^{Ik*} K^{IJ} m_d^{JJ} Z_{2p}^{-*}.$$

The next-to-leading corrections to $C_7(M_W)$ are found by taking diagrams from Figs. 14 and 15, adding one virtual gluon to them, and calculating their short-distance part. This has been done only in the SM case [21]. In the supersymmetric case, only contributions proportional to logarithms of superpartner masses are known [26], which is enough only for very heavy superpartners.

¹²It would not be the case for arbitrary MSSM parameters when extra operators in the effective theory could arise. However, so long as our assumptions from the beginning of this section are fulfilled, all these extra operators are negligible.

So long as the superpartners are heavy and their contributions to $C_7(M_W)$ are small (say, below 30%), then it does not really matter that the SUSY NLO corrections to $C_7(M_W)$ are unknown. The uncertainty is then dominated by SM sources anyway. However, if some of the SUSY contributions are big but cancel each other, so that the experimental $B \rightarrow X_s \gamma$ constraints [27] are fulfilled, then the lack of SUSY NLO corrections to $C_7(M_W)$ does matter. Such cancellations really do occur in sizable and interesting domains of the MSSM parameter space [28, 14]. This is why a calculation of the SUSY NLO corrections to $C_7(M_W)$ would be welcome.

In the results presented below, the complete Standard Model NLO formulae and values of parameters are used precisely as they stand in ref. [19]. As far as SUSY contributions to $C_7(M_W)$ and $C_8(M_W)$ are concerned, we have used only the available leading order results. The charged higgson and chargino contributions to $C_7(M_W)$ are separately assumed to have additional 10% uncertainty due to order $\alpha_s(M_W)/\pi$ corrections to them. These uncertainties are added in squares to the remaining errors. This way we have simulated growth of uncertainty in cases where large cancellations between SUSY contributions occur.

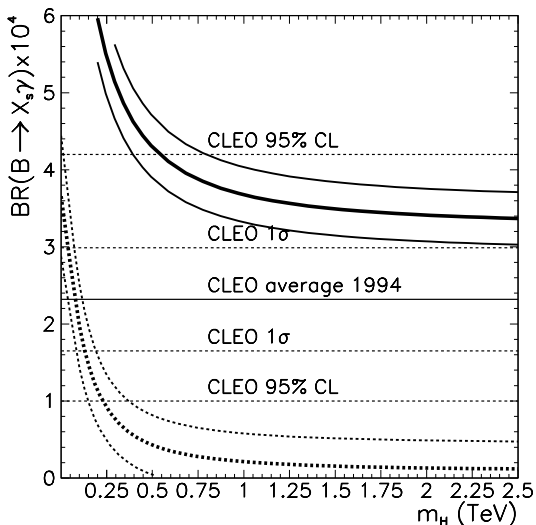


Figure 16: $Br[B \rightarrow X_s \gamma]$ as a function of the charged higgson mass.

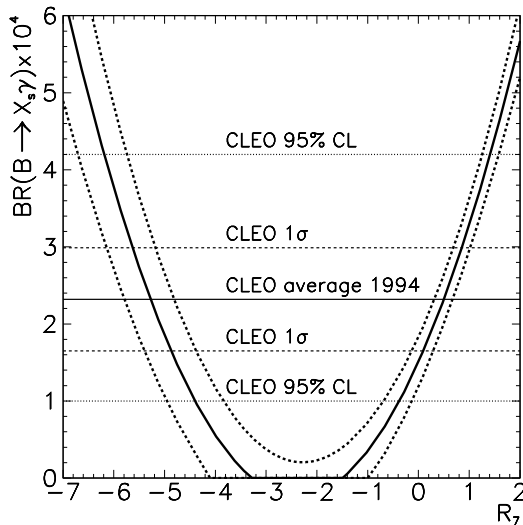


Figure 17: $Br[B \rightarrow X_s \gamma]$ as a function of R_7 .

Figure 16 presents two examples of how $Br[B \rightarrow X_s \gamma]$ depends on the charged higgson mass. Solid lines correspond to the case when all the superpartner masses are large (above 1 TeV). In this case, the MSSM results are the same as in the Two-Higgs-Doublet Model II. The value of $\tan \beta = 2$ was used. However, any larger value would give almost the same results, while for smaller $\tan \beta$, we would have an additional enhancement. The middle line corresponds to the central value, and the two remaining lines show the estimated uncertainty. For heavy charged higgson (well above 1 TeV), the curve approaches the SM result $Br[B \rightarrow X_s \gamma] = (3.28 \pm 0.33) \times 10^{-4}$. The horizontal lines show the CLEO 1σ error bar $(2.32 \pm 0.67) \times 10^{-4}$ as well as their 95% CL upper and lower bounds [27]. We can see that the theoretical prediction crosses the 95% CL upper line close to $M_{H^\pm} = 500$ GeV. This sets the lower bound on this mass in the considered MSSM scenario, and an absolute lower bound in the Two-Higgs-Doublet Model II.

Dashed lines in Fig. 16 correspond to another example. Here, chargino contributions are not negligible. We have taken $M_{\tilde{\chi}_1^\pm} = 90$ GeV, $m_{\tilde{T}_1} = 100$ GeV, $\tan \beta = 2$, $M_2/\mu = -5$ and $\theta_{LR} = 25^\circ$. All the squarks and sleptons except \tilde{T}_1 are assumed to be heavier than 1 TeV, which makes their contributions negligible. One can see that no lower bound on the charged higgson mass can be derived from $B \rightarrow X_s \gamma$ in this case. Actually, H^\pm has to be relatively light here in order to cancel the chargino contribution and bring the prediction back to the experimentally allowed range.

In the MSSM as well as in many other extensions of the Standard Model (in which the NLO corrections to $C_i(M_W)$ are unknown), extra contributions to $B \rightarrow X_s \gamma$ can be parameterized in terms of two parameters

$$R_7 = 1 + \frac{C_7^{(0)extra}(M_W)}{C_7^{(0)SM}(M_W)}, \quad R_8 = 1 + \frac{C_8^{(0)extra}(M_W)}{C_8^{(0)SM}(M_W)}. \quad (50)$$

Figure 17 presents the dependence of $Br[B \rightarrow X_s \gamma]$ on the parameter R_7 in the case when R_8 is set to unity. The meaning of various curves is the same as in Fig. 16: the middle one is the central value while the remaining two show the uncertainty. The horizontal lines are the experimental constraints. One can see that two ranges of R_7 are experimentally allowed. They correspond to two possible signs of the decay

amplitude: the same or opposite than in the SM.

The allowed ranges for R_7 are rather insensitive to R_8 , because $C_8(M_W)$ has little influence on the decay rate. For instance, shifting R_8 from 1 to 3 would affect the curves in Fig. 17 by less than the shown uncertainties. Thus, the presented plot allows to qualitatively test various extensions of the SM without the necessity of calculating the branching ratio itself – it is enough to calculate $C_7^{(0)}(M_W)$ only. The situation becomes more complex when contributions to R_8 are very large, as it may happen in some corners of the MSSM parameter space [6].

The existing measurement of $Br(B \rightarrow X_s \gamma)$ imposes already significant constraints on the MSSM parameter space. In order to understand these limits, it is important

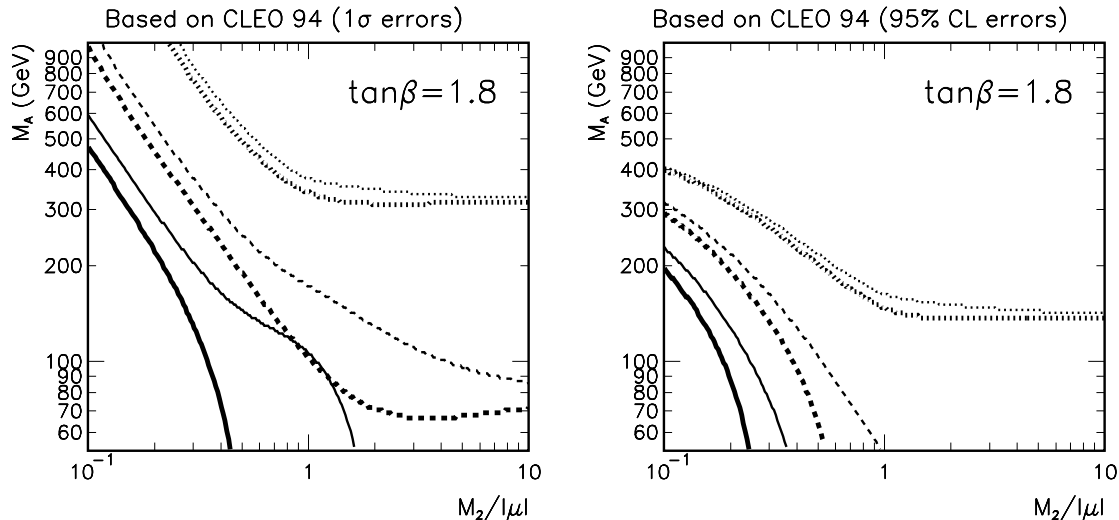


Figure 18: Lower limits on allowed M_A as a function of $M_2/|\mu|$, based on CLEO $Br(B \rightarrow X_s \gamma)$ measurement. Thick lines show limits for $\mu > 0$, thin lines for $\mu < 0$. Solid, dashed and dotted lines show limits for lighter stop and chargino masses $m_{\tilde{t}_1} = m_{\chi_{\pm 1}^0} = 90, 150$ and 300 GeV, respectively.

to remember that the charged Higgs and chargino-stop contributions to this process may have opposite signs. Since the actually measured value of $Br(B \rightarrow X_s \gamma)$ is close to the SM prediction, SUSY contributions must either be small or cancel each other to a large extent. Furthermore, large contributions to $Br(B \rightarrow X_s \gamma)$ are given by the Higgsino loops rather than gaugino exchanges. The content of lighter chargino

is determined by the M_2/μ parameter. In addition, the size of the chargino-stop contribution can be modified by changing the stop mixing angle θ_{LR} . We illustrate those effects in Figs. 18 and 19. Fig. 18 shows the lower limit on the allowed pseu-

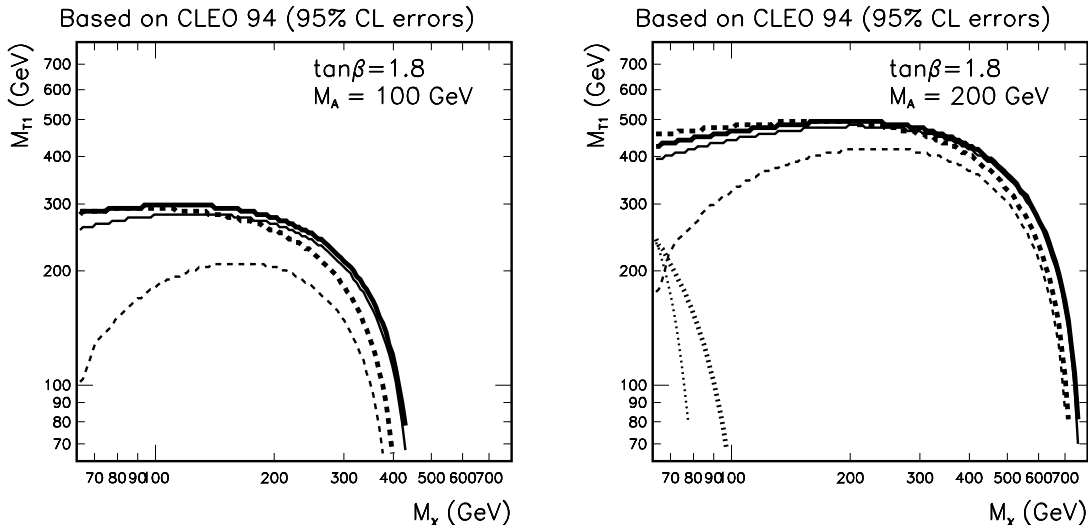


Figure 19: Upper bounds on $(m_{\tilde{T}_1}$ and $m_{\tilde{\chi}_1^\pm})$ for $\tan \beta = 1.8$ and $M_A = 100$ and 200 GeV. Thick lines show limits for $\mu > 0$, thin lines for $\mu < 0$. Dotted, dashed and solid lines show limits for $M_2/|\mu| = 0.1, 1$ and 10 , respectively.

doscalar Higgs boson mass M_A as a function of $M_2/|\mu|$ for three chosen values of lighter chargino and lighter stop masses. The charged Higgs boson mass is in one-to-one correspondence with M_A : At the tree level $M_{H^\pm}^2 = M_A^2 + M_W^2$. In Fig. 19, we plot the limits on lighter chargino and lighter stop mass for chosen M_A and $M_2/|\mu|$ values. In both plots we scan over θ_{LR} in the range $-60^\circ < \theta_{LR} < 60^\circ$.

Fig. 18 shows that if $M_2/|\mu|$ is small, so that lighter chargino consists predominantly of gaugino and its contribution to $Br(B \rightarrow X_s \gamma)$ is small, limits on M_A are quite strong. e.g. $M_A \geq \mathcal{O}(200 \text{ GeV})$ for $m_{\tilde{T}_1} = m_{\tilde{\chi}_1^\pm} = 90 \text{ GeV}$ (we take 95% errors of CLEO measurement). The limits decrease when $M_2/|\mu|$ increases and approximately saturate for $M_2/|\mu| \geq 1$. Similar effects are visible in Fig. 19 where upper bounds on $(m_{\tilde{T}_1}$ and $m_{\tilde{\chi}_1^\pm})$ are shown. For small $M_2/|\mu|$, very light stop and chargino are necessary to cancel the charged Higgs contribution. Thus, the corresponding upper limits on their masses are very strong. For large $M_2/|\mu|$, chargino

and stop even 2-3 times heavier than the charged Higgs are allowed.

5 Implications of the FCNC bounds for SUSY breaking and sfermion mass generation

We have already said in section 4 that the problem of achieving the necessary suppression of SUSY contributions to FCNC processes admits two broad classes of solutions (besides fine-tuning). One of them relies on the possibility that sfermions of the first two generations are much heavier than the usually expected scale of supersymmetry breaking $\mathcal{O}(1 \text{ TeV})$. In this case, the suppression of FCNC effects in the MSSM is achieved with essentially arbitrary flavour structure of squark mass matrices. The other possibility is that sfermion mass matrices at M_Z energy scale are indeed, for some reason, almost flavour conserving in the super-KM basis, and have approximately degenerate diagonal mass terms of the first two generation sfermions. Here, we would like to discuss and summarize various theoretical aspects and ideas behind these two general approaches to the FCNC problem in the MSSM.

Beginning with the possibility of heavy sfermions of the first two generations, one should stress (see e.g. [10]) that it is consistent with supersymmetry remaining the solution to the hierarchy problem. Indeed, the minimization of the Higgs potential in the MSSM gives

$$M_Z^2 = \frac{2}{\tan^2 \beta - 1} \left(M_{H^1}^2 + |\mu|^2 - (M_{H^2}^2 + |\mu|^2) \tan^2 \beta \right) \quad (51)$$

where M_{H^1} and M_{H^2} are the soft Higgs masses defined in eq. (3) and μ is defined in eq. (2). The hierarchy problem is avoided so long as we do not introduce large cancellations in eq. (51), after expressing M_{H^1} and M_{H^2} in terms of the soft masses at M_{GUT} . Using the appropriate RG equations one obtains

$$\begin{aligned} M_Z^2 \simeq & a_{H^1} M_{H^1}^2(M_{GUT}) + a_{H^2} M_{H^2}^2(M_{GUT}) + a_{QU} [(M_Q^2)^{33}(M_{GUT}) + (M_U^2)^{33}(M_{GUT}) \\ & - 2|\mu(M_Z)|^2 + a_{AA} [A_U^{33}(M_{GUT})]^2 + a_{AM} A_U^{33}(M_{GUT}) M_{1/2}(M_{GUT}) + a_{MM} M_{1/2}^2(M_{GUT})]. \end{aligned} \quad (52)$$

For $m_t = 175 \text{ GeV}$ and $\tan \beta = 1.65(2.2)$, the values of the coefficients are the following [29]: $a_{H^1} = 1.2(0.5)$, $a_{H^2} = 1.7(1.5)$, $a_{QU} = 1.5(1.1)$, $a_{AA} = 0.1(0.2)$,

$a_{AM} = -0.3(-0.7)$ and $a_{MM} = 15.0(10.8)$. The crucial observation is that to a very good approximation (see ref. [10] for corrections), the first two generation sfermion masses do not enter into the above expression for M_Z . The dominant role in this expression is played by the common gaugino mass $M_{1/2}$ at M_{GUT} and the third generation sfermion masses. The constraint on the first two generations (via D -term in the Lagrangian) is very weak and admits masses $m_{1,2} \sim \mathcal{O}(10 \text{ TeV})$. Thus, large non-universality with $m_{1,2} \sim \mathcal{O}(10 \text{ TeV})$ and $m_3 \leq 1 \text{ TeV}$ is consistent with the absence of large cancellations in the Higgs potential. On the other hand, we observe that $M_{1/2}$ and m_3 have to be rather small at M_{GUT} . In particular, large coefficient in eq. (52) requires very light chargino. The low energy stop mass parameters are actually even smaller than m_3 at M_{GUT} due to the running with large Y_t . Thus, the scenario with light chargino and stop is not unattractive. The discussed solution does not require any constraints on flavour off-diagonal entries in the (1,2) sector.

Another way to solve the FCNC problem in the MSSM is to embed this model into a high energy theory which assures small δ^{IJ} at the M_Z scale. Several ideas along these lines have been discussed in the literature. Generally speaking, this option correlates much stronger the FCNC problem with the theory of soft SUSY breaking and/or fermion mass generation.

Before going into further details we would like to address one interesting renormalization effect: Very small δ^{IJ} at M_Z do not necessarily imply that δ^{IJ} are small at M_{GUT} . Indeed, as it has been shown in ref. [30], there are QCD renormalization effects which increase only diagonal entries in the sfermion mass matrices. Consequently, they suppress δ^{IJ} . These effects can become dramatic when scalar masses at M_{GUT} are much smaller than $M_{1/2}$. Then even $\delta^{IJ} \sim \mathcal{O}(1)$ is acceptable in the squark sector at M_{GUT} . This could still happen with gaugino masses being $\mathcal{O}(M_Z)$. There are no absolute lower bounds on scalar masses at M_{GUT} . If they are much smaller than $M_{1/2}$, then this latter parameter sets the magnitude of physical masses for basically all the superpartners.

Such a scenario is not free of problems either. So long as no theoretical reason is found for $M_{1/2}$ being much larger than other soft SUSY breaking parameters at

M_{GUT} , this has to be understood as certain fine-tuning. Moreover, suppression of δ^{IJ} in the lepton sector is much less efficient because electroweak renormalization effects are smaller. One may conclude that although renormalization effects are helpful, they do not eliminate the flavour problem. If δ^{IJ} is small at the M_Z scale, we need a theory of flavour which assures it.

A simpler way to account for small δ^{IJ} at M_Z is to assure that the soft supersymmetry breaking scalar masses are generated as flavour diagonal and degenerate, and that the trilinear A -terms are proportional to the Yukawa couplings with a universal mass coefficient [31]. Thus, the absence of strong FCNC effects in SUSY would be explained by a particularly simple pattern of soft supersymmetry breaking (“universal soft terms”), with no correlation to the fermion mass generation. This scenario can be obtained under the assumption of dilaton dominance in the supergravity models for soft supersymmetry breaking [32]. However, deeper understanding of neither such a dominance nor the stabilization of the dilaton potential is available yet. Another possibility is gauge mediated supersymmetry breaking at low energies [33], which naturally leads to almost universal soft terms.

Quark-squark mass alignment is a different idea which relies on strong correlation between fermion and sfermion mass generation. Many different models of that type have been proposed. The most popular ones explore horizontal symmetries or an anomalous $U(1)$ symmetry [34].

Both options, if realized in an exact way, leave no room for flavour violation in the sfermion mass matrices, up to small $\mathcal{O}(K^{IJ})$ renormalization effects. However, in most “realistic” models of both types, there are interesting departures from the exact realization. For instance, in the supergravity models with Grand Unified groups, it is natural to assume universal soft terms at the Planck scale rather than at the GUT scale. The RG running down to the GUT scale generates flavour mixing in both the squark and slepton mass matrices at M_{GUT} . This gives interesting effects for $l^I \rightarrow l^J \gamma$ [35], within the reach of the forthcoming experiments. Moreover, the evolution down to low energies gives generically light stop, i.e. the scenario we have discussed in section 4.

Similar “inverse hierarchy” of sfermion masses (with respect to fermion ones) is also obtained in models with a $U(1)$ symmetry [36]. The quark-squark mass alignment is generically not perfect, and the FCNC effects are expected to be not much below the present experimental bounds.

6 Summary

There exist important bounds on new sources of FCNC in the MSSM. When the SUSY breaking scale is around 1 TeV, some of the flavour off-diagonal entries in the squark mass matrices have to be an order of magnitude lower than the diagonal ones. Most severe constraints exist in the left-right squark mixing sector. However, they could be considered dramatic only when flavour-conserving left-right mixing was generically large. Bounds on the squark mass degeneracy are in the range of few tens of percent even for the first two generations, so long as their masses are around 1 TeV. Thus, we conclude that the supersymmetric flavour problem is intriguing but perhaps not as severe as it has been commonly believed.

Restrictions on supersymmetric flavour violation have no immediate explanation in terms of the basic structure of the MSSM. They provide an important hint on its embedding into a more fundamental theory of soft supersymmetry breaking and fermion mass generation. Interesting effects in $\bar{K}^0 K^0$, $\bar{B}^0 B^0$ and particularly in $b \rightarrow s\gamma$ can be expected from light stop and chargino. Interesting effects can be expected in the lepton sector ($l^I \rightarrow l^J \gamma$), as well. Models of soft supersymmetry breaking which are consistent with the existing bounds leave room for such new effects. New sector of “precision experiments” (à la LEP) is welcome!

Note Added

The expressions for chargino contributions to $b \rightarrow s\gamma$ presented in our appendix allow to derive a bound on $(\delta_U^{23})_{LR}$. Requiring that the second term in eq. (A.10) gives smaller contribution to the amplitude than the Standard Model, we find

$$|(\delta_U^{23})_{LR}| \lesssim 12 \left(\frac{m_0}{1 \text{ TeV}} \right)^2 F, \quad (53)$$

where m_0 is the average up-squark mass, and the factor F is of order unity or larger. The explicit expression for F is

$$F = \sin\beta \left| x_1^2 f_1'(x_1) Z_{11}^{+*} Z_{21}^+ + x_2^2 f_1'(x_2) Z_{12}^{+*} Z_{22}^+ \right|^{-1}, \quad (54)$$

where $x_p = m_0^2/m_{\chi_p^\pm}^2$ and $f_1'(x)$ is the derivative of the function f_1 given below eq. (49). Even when $F = 1$, the bound on the r.h.s. of eq. (53) is smaller than unity (i.e. effective) only for the average squark mass below around 300 GeV.

The same bound holds for $(\delta_U^{13})_{LR}$, because we know from experiment that $b \rightarrow d\gamma$ does not have significantly larger rate than the SM prediction for $b \rightarrow s\gamma$. Bounds on $(\delta_U^{13})_{LR}$ and $(\delta_U^{23})_{LR}$ can be derived from chargino contributions to $\bar{B}^0 B^0$ mixing, too.

We thank Luca Silvestrini and Andrea Romanino for bringing bounds on $(\delta_U^{13})_{LR}$ and $(\delta_U^{23})_{LR}$ to our attention.

Acknowledgements

We thank Piotr Chankowski, Antonio Masiero and Luca Silvestrini for helpful discussions.

This work was supported in part by the Polish Committee for Scientific Research under grants 2 P03B 040 12 (1997-98) and 2 P03B 180 09 (1995-97) and by EC contract HCOMP CT92004. M.M. was supported in part by Schweizerischer Nationalfonds. J.R. was supported in part by Alexander von Humboldt Stiftung.

Appendix A

As an example, we discuss in more detail the chargino-(up squark) contribution to $b \rightarrow s\gamma$ decay rate. This contribution is proportional to the quantity $C_7^{(0)\chi^\pm}(M_W)$ given in eq. (49). In order to obtain the expression for $C_7^{(0)\chi^\pm}(M_W)$ in the mass insertion approximation discussed in Sec. 3, we expand the exact formulae (49) up to the first order in the physical up-squark mass splitting:

$$m_{\tilde{U}_i}^2 = m_0^2 + \delta m_{\tilde{U}_i}^2 \quad (A.1)$$

The functions f_1 and f_2 can be expanded around the average mass m_0^2 as

$$\begin{aligned} f_1\left(\frac{m_{\tilde{U}_i}^2}{m_{\chi_p^\pm}^2}\right) &\approx f_1\left(\frac{m_0^2}{m_{\chi_p^\pm}^2}\right) + \frac{m_{\tilde{U}_i}^2 - m_0^2}{m_{\chi_p^\pm}^2} f_1'\left(\frac{m_0^2}{m_{\chi_p^\pm}^2}\right) \\ &= \alpha_1^p + \beta_1^p m_{\tilde{U}_i}^2, \end{aligned} \quad (\text{A.2})$$

where

$$\alpha_1^p = f_1\left(\frac{m_0^2}{m_{\chi_p^\pm}^2}\right) - \frac{m_0^2}{m_{\chi_p^\pm}^2} f_1'\left(\frac{m_0^2}{m_{\chi_p^\pm}^2}\right) \quad (\text{A.3})$$

$$\beta_1^p = \frac{1}{m_{\chi_p^\pm}^2} f_1'\left(\frac{m_0^2}{m_{\chi_p^\pm}^2}\right), \quad (\text{A.4})$$

and similarly for the function f_2 . After such expansion, eq. (49) may be rewritten in the form

$$\begin{aligned} C_7^{(0)\chi^\pm}(M_W) &= \frac{1}{K_{ts}^* K_{tb}} \sum_{p=1}^2 \frac{M_W^2}{m_{\chi_p^\pm}^2} \left\{ -\frac{1}{6} \alpha_1^p \sum_{i=1}^6 A_{i2}^{p*} A_{i3}^p - \frac{1}{6} \beta_1^p \sum_{i=1}^6 A_{i2}^{p*} A_{i3}^p m_{\tilde{U}_i}^2 \right. \\ &\quad \left. + \frac{m_{\chi_p^\pm}^2}{3m_b} \left[\alpha_2^p \sum_{i=1}^6 A_{i2}^{p*} B_{i3}^p + \beta_2^p \sum_{i=1}^6 A_{i2}^{p*} B_{i3}^p m_{\tilde{U}_i}^2 \right] \right\} + \mathcal{O}((\delta m^2/m_0^2)^2). \end{aligned} \quad (\text{A.5})$$

Sums over i in the eq. (A.5) can be calculated using unitarity of the matrix Z_U and eq. (12)

$$\sum_{k=1}^6 Z_U^{ik} Z_U^{jk*} = \hat{1}^{ij} \quad (\text{A.6})$$

$$\sum_{k=1}^6 Z_U^{ik} Z_U^{jk*} m_{\tilde{U}_i}^2 = (\mathcal{M}_{\tilde{U}}^2)^{ij} \quad (\text{A.7})$$

Evaluating the four sums appearing in eq. (A.5) gives the following results:

$$\sum_{i=1}^6 A_{i2}^{p*} A_{i3}^p = \frac{1}{2M_W^2 \sin^2 \beta} |Z_{2p}^+|^2 [K^\dagger m_u^2 K]_{23} \quad (\text{A.8})$$

$$\sum_{i=1}^6 A_{i2}^{p*} B_{i3}^p = 0 \quad (\text{A.9})$$

$$\begin{aligned} \sum_{i=1}^6 A_{i2}^{p*} A_{i3}^p m_{\tilde{U}_i}^2 &= |Z_{1p}^+|^2 [K^\dagger (M_{\tilde{U}}^2)_{LL} K + K^\dagger m_u^2 K]_{23} \\ &\quad - \frac{1}{\sqrt{2} M_W \sin \beta} Z_{1p}^{+*} Z_{2p}^+ [K^\dagger (M_{\tilde{U}}^2)_{LR} m_u K - \mu \cot \beta K^\dagger m_u^2 K]_{23} \\ &\quad - \frac{1}{\sqrt{2} M_W \sin \beta} Z_{1p}^+ Z_{2p}^{+*} [K^\dagger m_u (M_{\tilde{U}}^2)_{LR}^\dagger K - \mu^* \cot \beta K^\dagger m_u^2 K]_{23} \end{aligned}$$

$$+ \frac{1}{2M_W^2 \sin^2 \beta} |Z_{2p}^+|^2 \left[K^\dagger m_u (M_{\tilde{U}}^2)_{RR} m_u K + K^\dagger m_u^4 K \right]_{23} \quad (\text{A.10})$$

$$\begin{aligned} \sum_{i=1}^6 A_{i2}^{p*} B_{i3}^p m_{\tilde{U}_i}^2 &= -\frac{m_b}{\sqrt{2} M_W \cos \beta} Z_{1p}^{+*} Z_{2p}^{-*} \left[K^\dagger (M_{\tilde{U}}^2)_{LL} K + K^\dagger m_u^2 K \right]_{23} \\ &+ \frac{m_b}{M_W^2 \sin 2\beta} Z_{2p}^{+*} Z_{2p}^{-*} \left[K^\dagger m_u (M_{\tilde{U}}^2)_{LR}^\dagger K - \mu^* \cot \beta K^\dagger m_u^2 K \right]_{23} \end{aligned} \quad (\text{A.11})$$

Inserting the above sums into the eq. (A.5), we obtain an approximate expression for the chargino contribution to $b \rightarrow s\gamma$ decay amplitude expressed in terms of the initial squark mass matrices.

As seen in eqs. (A.8)–(A.11), there are many terms in this contribution which survive in the limit of flavour-conserving squark mass matrices. The FCNC effects we have discussed in section 4 originate from these terms.

An important observation is that, as follows from eq. (11), $(M_{\tilde{U}}^2)_{LL} = K(M_{\tilde{D}}^2)_{LL}K^\dagger$. After inserting this relation into eqs. (A.8)–(A.11), we come to an immediate conclusion that, as far as the left squarks are concerned, chargino contributions to $b \rightarrow s\gamma$ are directly sensitive to the structure of down (not up!) left squark mass matrix (as the diagrams with gluino and neutralino exchanges are). The situation with right squark mass matrices is more complicated: In the expressions for chargino contributions, they are multiplied by quark masses and the KM matrices, which causes that the final result is sensitive to the linear combination of various off-diagonal entries and also to the splitting of the diagonal elements. However, most of these terms are suppressed by light quark masses.¹³ For instance, $K^\dagger m_u (M_{\tilde{U}}^2)_{RR} m_u K$ can be written as

$$\begin{aligned} K^\dagger m_u (M_{\tilde{U}}^2)_{RR} m_u K &\approx m_t^2 (M_{\tilde{U}}^2)_{RR}^{33} \begin{pmatrix} 0 & 0 & K^{31*} \\ 0 & 0 & K^{32*} + \frac{m_c (M_{\tilde{U}}^2)_{RR}^{23}}{m_t (M_{\tilde{U}}^2)_{RR}^{33}} \\ K^{31} & K^{32} + \frac{m_c (M_{\tilde{U}}^2)_{RR}^{32}}{m_t (M_{\tilde{U}}^2)_{RR}^{33}} & 1 \end{pmatrix} \\ &+ \text{smaller terms} \end{aligned} \quad (\text{A.12})$$

Therefore $\left(K^\dagger m_u (M_{\tilde{U}}^2)_{RR} m_u K \right)_{23} \approx m_t^2 (M_{\tilde{U}}^2)_{RR}^{33} K^{32*} + m_c m_t (M_{\tilde{U}}^2)_{RR}^{23}$ is basically sensitive only to the elements $(M_{\tilde{U}}^2)_{RR}^{23}, (M_{\tilde{U}}^2)_{RR}^{33}$.

¹³ The only exception is the second term in eq. (A.10) which gives a bound on $(\delta_{\tilde{U}}^{23})_{LR}$.

Another (and most obvious) simplification of eqs. (A.8-A.11) is achieved by neglecting light quark masses in

$$(K^\dagger m_u^n K)_{23} \approx K^{32*} K^{33} m_t^n = K_{ts}^* K_{tb} m_t^n, \quad n = 2, 4. \quad (\text{A.13})$$

The observation that chargino contributions to the $b \rightarrow s\gamma$ depend on the down, not up, left squark mass matrix may be generalized to other processes. One always finds that chargino, neutralino and gluino contributions to the processes involving down quarks in the initial and final states are sensitive to the structure of the left down squark matrices only. It follows from the structure of the up-squark mass matrix (eq. (7)) and $u\tilde{D}\chi$ vertex shown in Fig. 1. One can verify this by writing the matrix Z_U in the form

$$Z_U = \begin{pmatrix} K & 0 \\ 0 & 1 \end{pmatrix} X_U \quad (\text{A.14})$$

The new “rotated” diagonalization matrix X_U is defined by the following condition:

$$(\mathcal{M}_{\tilde{U}}^2)^{diag} = X_U^\dagger \mathcal{M}_{X\tilde{U}}^2 X_U \quad (\text{A.15})$$

where $\mathcal{M}_{X\tilde{U}}^2$ is explicitly dependent on the left down squark mass matrix $(M_D^2)_{LL}$

$$\mathcal{M}_{X\tilde{U}}^2 = \begin{pmatrix} (M_D^2)_{LL} + K^\dagger m_u^2 K - \frac{\cos 2\beta}{6} (M_Z^2 - 4M_W^2) \hat{1} & K^\dagger \left((M_U^2)_{LR} - \cot \beta \mu m_u \right) \\ \left((M_U^2)_{LR}^\dagger - \cot \beta \mu^* m_u \right) K & (M_U^2)_{RR} + m_u^2 + \frac{2\cos 2\beta}{3} M_Z^2 \sin^2 \theta_W \hat{1} \end{pmatrix} \quad (\text{A.16})$$

The $u\tilde{D}\chi$ vertex written in terms of X_U takes the form

$$i \left[\left(-g_2 X_U^{Ji*} Z_{1j}^+ + K^{JI} Y_u^J X_U^{(J+3)i*} Z_{2j}^+ \right) P_L - Y_d^I X_U^{Ji*} Z_{2j}^- P_R \right] \quad (\text{A.17})$$

In this expression, the KM matrix occurs only multiplied by the up-quark Yukawa couplings which originate from the higgsino–(right squark) interactions.

Similarly, one can prove that processes involving up quarks in the initial and final states (like $\bar{D}^0 D^0$ mixing) are sensitive only to the structure of the left up squark mass matrix.

References

- [1] M.J. Duncan, *Nucl. Phys.* **B221** (1983) 285;
J.F. Donoghue, H.P. Nilles and D. Wyler, *Phys. Lett.* **B128** (1983) 55;
A. Boquet, J. Kaplan and C.A. Savoy, *Phys. Lett.* **B148** (1984) 69.
- [2] J. Rosiek, *Phys. Rev.* **D41** (1990) 3464; *erratum* hep-ph/9511250.
- [3] F. Gabbiani and A. Masiero, *Nucl. Phys.* **B322** (1989) 235;
J.S. Hagelin, S. Kelley and T. Tanaka, *Nucl. Phys.* **B415** (1994) 293.
- [4] F. Gabbiani, E. Gabrielli, A. Masiero and L. Silvestrini, *Nucl. Phys.* **B477** (1996) 321.
- [5] A.J. Buras, plenary talk given at the ICHEP96 conference, Warsaw, July 1997 (hep-ph/9610461) and references therein.
- [6] M. Ciuchini, E. Gabrielli and G.F. Giudice, *Phys. Lett.* **B388** (1996) 353, *Phys. Lett.* **B393** (1997) 489(E).
- [7] A. Ali, G.F. Giudice and T. Mannel, *Z. Phys.* **C67** (1995) 417.
- [8] P. Cho, M. Misiak and D. Wyler, *Phys. Rev.* **D54** (1996) 3329.
- [9] Y. Grossman, Y. Nir, R. Rattazzi, this volume (hep-ph/9701231).
- [10] S. Dimopoulos and G.F. Giudice, *Phys. Lett.* **B357** (1995) 573;
M. Carena et al., preprint CERN-Th/96-241 (hep-ph/9612261), to appear in *Nucl. Phys. B*.
- [11] T. Appelquist and J. Carrazzone, *Phys. Rev.* **D11** (1975) 2856.
- [12] Particle Data Group, *Phys. Rev.* **D54** (1996) 1.
- [13] P.H. Chankowski and S. Pokorski *Phys. Lett.* **B366** (1996) 188.
- [14] P.H. Chankowski and S. Pokorski *Nucl. Phys.* **B475** (1996) 3.

- [15] A.J. Buras, M Jamin and P.H. Weisz, *Nucl. Phys.* **B347** (1990) 491;
S. Herrlich and U. Nierste, *Nucl. Phys.* **B419** (1994) 292, *Phys. Rev.* **D52**
(1995) 6505.
- [16] L. Wolfenstein, *Phys. Rev. Lett.* **51** (1983) 1945.
- [17] G.C. Branco, G.C. Cho, Y. Kizukuri and N. Oshimo, *Phys. Lett.* **B337** (1994)
316, *Nucl. Phys.* **B449** (1995) 483;
G.C. Branco, W. Grimus and L. Lavoura, *Phys. Lett.* **B380** (1996) 119;
A. Brignole, F. Feruglio and F. Zwirner, *Z. Phys.* **C71** (1996) 679;
J. Rosiek, talk given at the ICHEP96 conference, Warsaw, July 1996.
- [18] A. J. Buras, M. Misiak, M. Münz, and S. Pokorski, *Nucl. Phys.* **B424** (1994)
374.
- [19] K. Chetyrkin, M. Misiak and M. Münz, preprint ZU-TH 24/96 (hep-
ph/9612313), to appear in *Phys. Lett. B*.
- [20] C. Greub, T. Hurth and D. Wyler, *Phys. Lett.* **B380** (1996) 385, *Phys. Rev.*
D54 (1996) 3350.
- [21] K. Adel and Y.P. Yao, *Phys. Rev.* **D49** (1994) 4945.
- [22] A. Ali and C. Greub, *Phys. Lett.* **B361** (1995) 146.
- [23] A.F. Falk, M. Luke and M. Savage, *Phys. Rev.* **D49** (1994) 3367.
- [24] M. Neubert, *Phys. Rev.* **D49** (1994) 4623
- [25] S. Bertolini, F. Borzumati, A. Masiero and G. Ridolfi, *Nucl. Phys.* **B353** (1991)
591.
- [26] H. Anlauf, *Nucl. Phys.* **B430** (1994) 245.
- [27] M.S. Alam et al., *Phys. Rev. Lett.* **74** (1995) 2885.
- [28] R. Barbieri and G.F. Giudice, *Phys. Lett.* **B309** (1993) 86;
R. Garisto and J.N. Ng, *Phys. Lett.* **B315** (1993) 372.

- [29] P.H. Chankowski and S. Pokorski, preprint CERN-TH/97-28 (hep-ph/9702431).
- [30] M. Dine, A. Kagan and S. Samuel, *Phys. Lett.* **B243** (1990) 250;
 A. Brignole, L.E. Ibañez and C. Muñoz, *Nucl. Phys.* **B422** (1994) 125;
 D. Choudhury et al., *Phys. Lett.* **B342** (1995) 180;
 P. Brax and M. Chemtob, *Phys. Rev.* **D51** (1995) 6550;
 P. Brax and C.A. Savoy, *Nucl. Phys.* **B** (1995) ;
 B. de Carlos, J.A. Casas and J.M. Moreno, *Phys. Rev.* **D53** (1996) 6398.
- [31] S. Dimopoulos and H. Georgi, *Nucl. Phys.* **B193** (1981) 150;
 H.P. Nilles, M. Srednicki and D. Wyler, *Phys. Lett.* **B120** (1983) 346.
- [32] R. Barbieri, J. Louis and M. Moretti, *Phys. Lett.* **B312** (1993) 451.
- [33] M. Dine, W. Fischler and M. Srednicki *Nucl. Phys.* **B189** (1981) 575;
 S. Dimopoulos and S. Raby *Nucl. Phys.* **B192** (1981) 353;
 L. Alvarez-Gaumé, M. Claudson and M. Wise *Nucl. Phys.* **B207** (1982) 96;
 M. Dine and A. Nelson, *Phys. Rev.* **D48** (1993) 1277;
 M. Dine, A. Nelson and Y. Shirman, *Phys. Rev.* **D51** (1995) 1362;
 M. Dine, A. Nelson, Y. Nir and Y. Shirman, *Phys. Rev.* **D53** (1996) 2658.
- [34] C.D. Froggatt and H.B. Nielsen, *Nucl. Phys.* **B147** (1979) 277, *Nucl. Phys.* **B164** (1979) 144;
 J. Harvey, P. Ramond and D. Reiss, *Phys. Lett.* **B92** (1980) 309;
 S. Dimopoulos, *Phys. Lett.* **B129** (1983) 417;
 C. Wetterich, *Nucl. Phys.* **B261** (1985) 461;
 A. Farragi, *Phys. Lett.* **B278** (1992) 131;
 Y. Nir and N. Seiberg, *Phys. Lett.* **B309** (1993) 337;
 M. Leurer, Y. Nir and N. Seiberg, *Nucl. Phys.* **B420** (1994) 468;
 L. Ibañez and G.G. Ross, *Phys. Lett.* **B332** (1994) 100;
 P. Binetruy and P. Ramond, *Phys. Lett.* **B350** (1995) 49;
 P. Binetruy and E. Dudas, *Nucl. Phys.* **B442** (1995) 21;

- V. Jain and R. Shrock, *Phys. Lett.* **B352** (1995) 83;
E. Dudas, S. Pokorski and C.A. Savoy, *Phys. Lett.* **B356** (1995) 45;
Y. Nir, *Phys. Lett.* **B354** (1995) 107.
- [35] S. Bertolini and A. Masiero, *Phys. Lett.* **B174** (1986) 343;
R. Barbieri and L.J. Hall, *Phys. Lett.* **B338** (1994) 212;
R. Barbieri, L.J. Hall and A. Sturmia, *Nucl. Phys.* **B445** (1995) 219, *Nucl. Phys.* **B449** (1995) 437;
L.J. Hall, V.A. Kostelecky and S. Raby, *Nucl. Phys.* **B267** (1986) 415.
- [36] E. Dudas and C. Savoy, *Phys. Lett.* **B369** (1996) 255;
E. Dudas, Ch. Grojean, S. Pokorski and C. Savoy *Nucl. Phys.* **B481** (1996) 85.